Master's Thesis

CRASY: The High-Resolution Pure Rotational Raman Spectra of trans-1,3-butadiene and Its Isotopologues in the Vibrational Ground State

Begüm Rukiye Özer

Department of Chemistry

Graduate School of UNIST

2019

CRASY: The High-Resolution Pure Rotational Raman Spectra of trans-1,3-butadiene and Its Isotopologues in the Vibrational Ground State

A thesis
submitted to the Graduate School of UNIST
in partial fulfillment of the
requirements for the degree of
Master of Science

Begüm Rukiye Özer

12/13/2018
Approved by

_____

Advisor
Thomas Schultz

CRASY: The High-Resolution Pure Rotational Raman Spectra of trans-1,3-butadiene and Its Isotopologues in the Vibrational Ground State

Begüm Rukiye Özer

This certifies that the thesis of Begüm Rukiye Özer

is approved.

01/09/2019

_____

Advisor: Thomas Schultz

_____

Thomas Schultz

_____

Yung-Sam Kim

_____

Oh-Hoon Kwon

CONTENTS

Abstract

Trans-1,3-butadiene was investigated by Correlated Rotational Alignment Spectroscopy (CRASY) in which pure rotational Raman information coupled to ion mass information. The rotational Raman spectra with a broad spectral bandwidth of 500 GHz were calibrated to a GPS stabilized external clock that enhanced the high accuracy in rotational constants. . Opto-mechanical delay stage, sparse sampling and pulse jumping settled CRASY into high resolution spectroscopic regime. We performed an analysis of the gas-phase rotational Raman spectrum of butadiene (BD) and its most abundant isotopologues of *1-^{13}C-BD* and *2-^{13}C-BD*. In this work, we advanced an order of magnitude better rotational constants for main BD isotope. The rotational constants of pure *2-^{13}C-BD* were also revealed for the first time.

1. Introduction

1.1.Rotational Spectroscopy

Rotational spectroscopy provides information on the geometry of molecules by predicting bond lengths and bond angles. To carry out the analysis of rotational spectra, moments of inertia should be calculated. The rotational structure can be interpreted in terms of the moments of inertia for each axis. The molecule of interest of this paper is butadiene, so the focus will be on the asymmetric top molecules throughout this paper. An asymmetric molecule has three different moments of inertia with the axes chosen as $I_c < I_b < I_a$. By introducing the rotational constants with respect to each moment of inertia,

$$A = \frac{\hbar}{4\pi c I_a} \ , \ B = \frac{\hbar}{4\pi c I_b} \text{ and } C = \frac{\hbar}{4\pi c I_c}$$

where ħ is the Planck's constant. Therefore, the energy of an asymmetric rotor can be expressed as,

$$E(a,b,c) = \frac{AP_a^2 + BP_b^2 + CP_c^2}{\hbar^2}$$

where P_a, P_b and P_c are the components of the angular momentum along the principle inertia axes a, b and c. [3]

So far, the molecules were treated as rigid rotors. However, there is a distortional force acting on molecules upon their rotational motion and this force also affects the moments of inertia of the molecule. There are three centrifugal distortion constants; D_j acts on $J^2(J+1)^2$ quartic centrifugal distortion, D_k acts on K^4 quartic centrifugal distortion, and D_{jk} acts on $J(J+1)K^2$ quartic centrifugal distortion. Higher distortion moments exist but are ignored here.

The rotational quantum numbers J and K are used to describe the rotational energy of rotational transitions. J describes the total angular momentum. K is the projection angular quantum number that indicates the component of J on the principal axis, as shown in Figure 1.

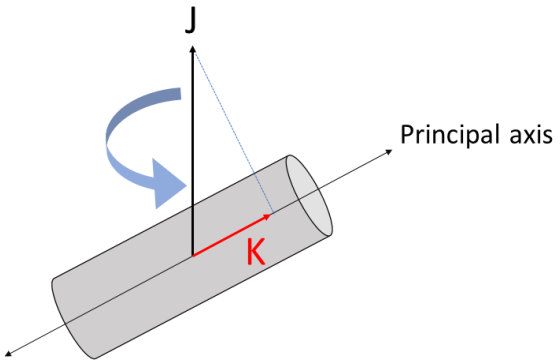

Figure 1. The scheme illustrating the quantum numbers of J and K. K quantum number is the projection of the total angular quantum number J on the principal axis.

The origin of spectral lines in a rotational spectrum stem from the transitions occurring from one rotational energy state to another. Not all transitions between all rotational states can occur. The allowed and forbidden transitions are expressed by the selection rules. The shape of the spectrum then is inferred by the population of states and the transition moments for allowed transitions.
The selection rules for Raman excitation of rotational transitions in asymmetric top molecules are ΔJ=0, ± 1, ±2 and ΔK=0, ±2. [1,2,3]

The spectral intensity is determined by the probability of that transition to occur. This probability is proportional to the population of the initial state of the transition and the degeneracy of the rotational states. By considering only J quantum number for the simplicity, the population is expressed by the Boltzmann distribution [4].

$$\text{Probability } \sim (2J+1)e^{\frac{-E_j}{kT}}$$

and the degeneracy is given as,

$$\text{Degeneracy } \sim (2J+1)$$

where E_j is the energy of the rotational transition, k is the Boltzmann constant and T is the absolute temperature. A transition intensity is directly proportional to the degeneracy and to the Boltzmann probability of the initial state. The above terms are more complicated for an asymmetric top molecule but were not discussed here for the fact that all the calculations were carried out by a simulation program called PGOPHER. [20]

Nuclear spin is another factor that effects the appearance of a spectrum. The Pauli principle [6] requires the total wavefunction to be antisymmetric with respect to an exchange.

$$\psi_{total} = \psi_{electronic}\psi_{vibrational}\psi_{rotational}\psi_{spin} \text{ (= antisymmetric)}$$

The electronic ground state and vibrational ground state has an even wavefunctions. Hence, the product of the rotational wavefunction and the nuclear spin wavefunction must be antisymmetric.

The spectral resolution is limited by the Heisenberg uncertainty [5],

$$\Delta E.\Delta t \geq \hbar$$

Therefore, the resolution ΔE of the frequency-domain spectrum is inversely proportional to the measurement time Δt. The longer the measurement, the better the resolution we can get.

1.2.Butadiene

Conjugation is a concept that describes the delocalization of electrons in the π-orbitals, resulting in higher stability and lower total energy. Butadiene (BD) is the simplest conjugated diene with a point group symmetry of C_{2h}. The molecular structure is shown in Figure 2. BD is a near-prolate asymmetric top molecule with a Ray's asymmetry parameter of κ = -0.9786 [21] (where $\kappa = \frac{2B-A-C}{A-C}$ and κ = -1 indicates the molecule to be a prolate symmetric top). BD has no permanent dipole moment due to its molecular symmetry, therefore, it is not accessible by microwave spectroscopy. However, the high polarization anisotropy of the delocalized pi-electrons makes BD a good candidate for rotational Raman excitation.

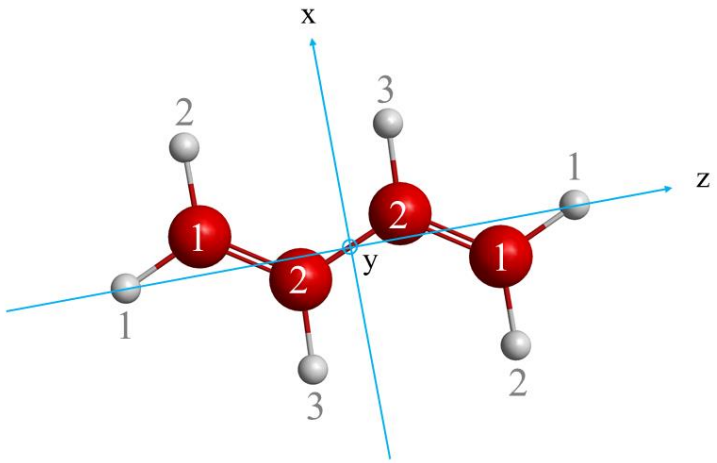

Figure 2. Molecular structure and atomic labelling of BD. Labelling of hydrogen and carbon atoms is performed according to the distance from the inversion of symmetry.

Butadiene has five major heavy isotopes, 1– ^{2}D, 2– ^{2}D, 3– ^{2}D, 1 – ^{13}C, 2 – ^{13}C shown in Figure 3. The probability of observing deuterated BD and ^{13}C substituted BD is 6 x 0.0115% and 4 x 1.1%, respectively. Therefore, deuterated isotopes can be neglected in the interpretation of the lines in the spectrum. Hence, the rotational spectra in Figure 17 were assigned to the most abundant isotopes of 1 – ^{13}C and 2 – ^{13}C.

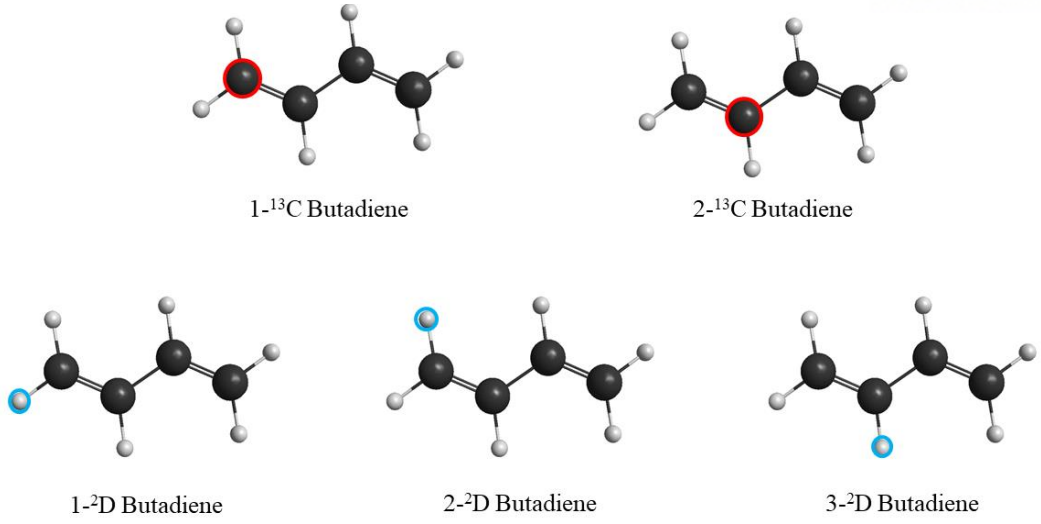

Figure 3. The most abundant heavy isotopes of BD.

The interaction of BD with the electric field components of the laser, as shown in Figure 4a, is dependent on the angle θ between the electric field and the principle axis of the molecule. It is maximized at $\theta=0^0$ and minimized at $\theta=90^0$. Figure 4b illustrates the energy of BD with its angle dependent character. BD has no dipole moment due to its molecular symmetry, however, the electric field can distort the electron cloud along the molecular axis and induce a dipole moment. BD molecules in gas phase rotate freely. Upon a non-adiabatic rotational Raman excitation with a linearly polarized IR pulse, the induced dipole moments are aligned along the electric field direction of the pulse. They then rotate coherently with a new angular momentum. The rotational motion occurs in the GHz to THz regime, which corresponds to a period of greater than picoseconds. For BD, the rotational periods are greater than 4 ps (≈ 250 GHz) ~ 40 ps (≈ 25 GHz) under the condition of < 10 K.

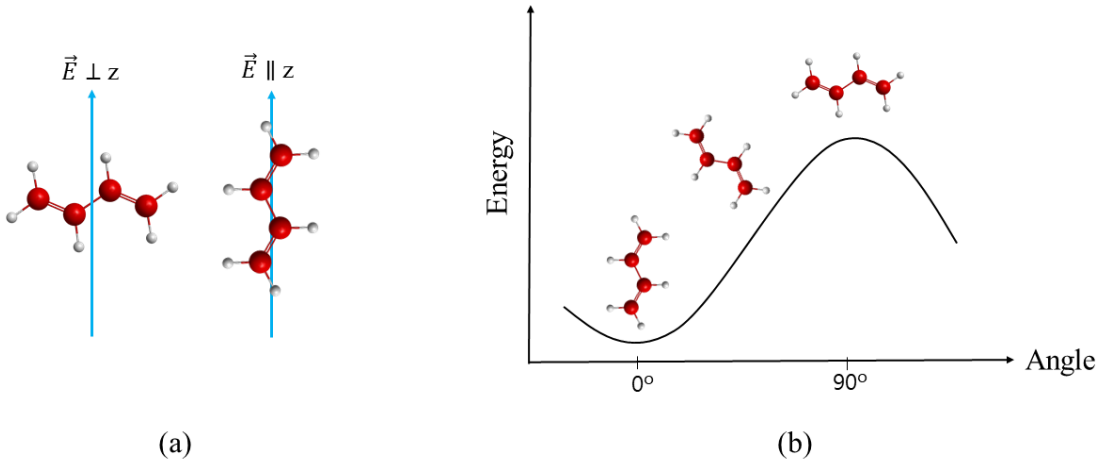

Figure 4. (a-left) The smallest interaction is obtained when the principle axis of the molecule is perpendicular to the electric field component of the laser. (a-right) The largest interaction is obtained when the principle axis of BD is parallel to the electric field component of the laser. (b) Energy diagram with respect to the angle between the electric field component of the pump laser and the principle axis of BD.

The rotational motion can be observed by rotational coherence spectroscopy (RCS) [8]. RCS is a time-domain spectroscopic technique that provides precise structural information of isolated species by monitoring modulations of quantized rotational motion. A polarized ultrashort laser pulse (ps duration) creates an initial alignment of molecular dipoles of gas phase molecules. Subsequent manifestation of alignment, due to the dephasing and rephasing of the rotational wavefunctions, can be observed by a probe pulse (fs duration) as a function of time.

Resonance enhanced multiphoton ionization (REMPI) is an ionization method, in which more than one photon is absorbed by the molecule to be ionized. [9] UV light is broadly used for this purpose. REMPI uses the resonant intermediate excited states to achieve efficient ionization with a longer wavelength (lower E) laser source. The evolution of the rotational wave packet can be monitored in the time-domain using REMPI, because the excitation dipole moment needs to be aligned correctly to observe REMPI signals.

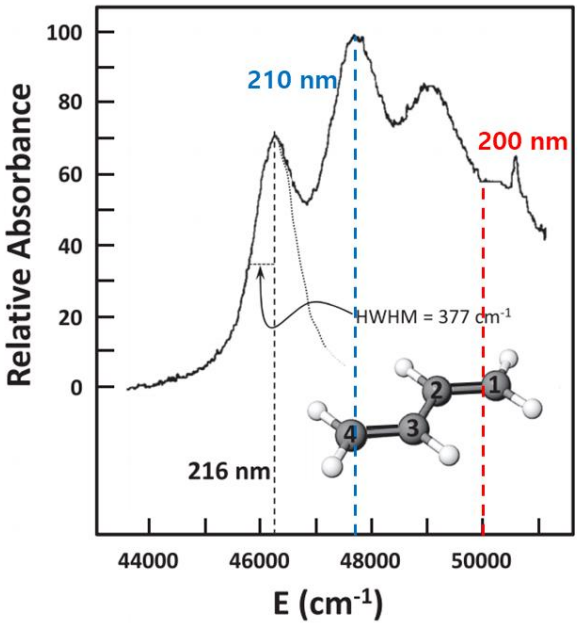

Figure 5. The UV absorption spectrum of trans-1,3-butadiene in the region of its π-π* transition. The transition is from the $S_0(1^1A_g)$ ground state (HOMO) to the bright $S_2(^1B_u)$ state (LUMO). [10]

BD shows an UV absorption spectrum due to a π-π* transition as shown in Figure 5. [10] The broad absorption band ranges from 44000 cm^{-1} (227 nm) to 51000 cm^{-1} (196 nm). The maximum absorption is around 47600 cm^{-1} (210 nm). The electronic excitation can be performed with 200 nm light, which is the forth harmonic of the Ti:Sa laser fundamental wavelength of 800 nm. By utilizing REMPI, ionization of BD can be achieved with a 200 nm laser beam.

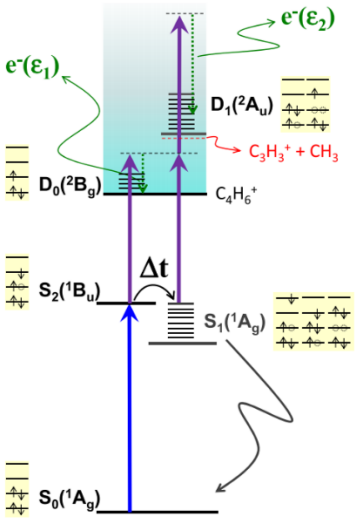

Figure 6. The electronic states, occupancy of π electron orbitals, energetics and excited state dynamics in BD, C_4H_6. [10]

UV laser light excites a π-electron from the $S_0(1^1A_g)$ ground state to the $S_2(^1B_u)$ excited state. This transition is the HOMO-LUMO transition. Due to ultrafast non-adiabatic dynamics, the $S_2(1^1B_u)$ excited state quickly relaxes into the lower lying $S_1(2^1A_g)$ state by internal conversion. In reference [10] (Figure 6), the bright $S_2(1^1B_u)$ state is probed by single photon ionization, where $S_1(2^1A_g)$ state is probed by two-photon ionization. In our CRASY experiment, the bright $S_2(1^1B_u)$ state serves as resonant intermediate state and is ionized by another 200 nm photon.

1.3.CRASY

Correlated Rotational Alignment Spectroscopy (CRASY) [11,12,13] is a mass-selective RCS technique that probes ground state rotational Raman excitation with femtosecond two-photon ionization (REMPI). This correlates rotational information with mass information. Figure 7 illustrates the CRASY experiment. In step A, an 800 nm IR pump pulse excites the rotational states by coherent Raman excitation in the vibrational ground state. In step B, a 200 nm UV probe pulse (generated by forth harmonic generation) excites molecules from the electronic ground state $S_0(1^1A_g)$ to the electronic excites state $S_2(^1B_u)$, followed by ionization to a final ionic state.

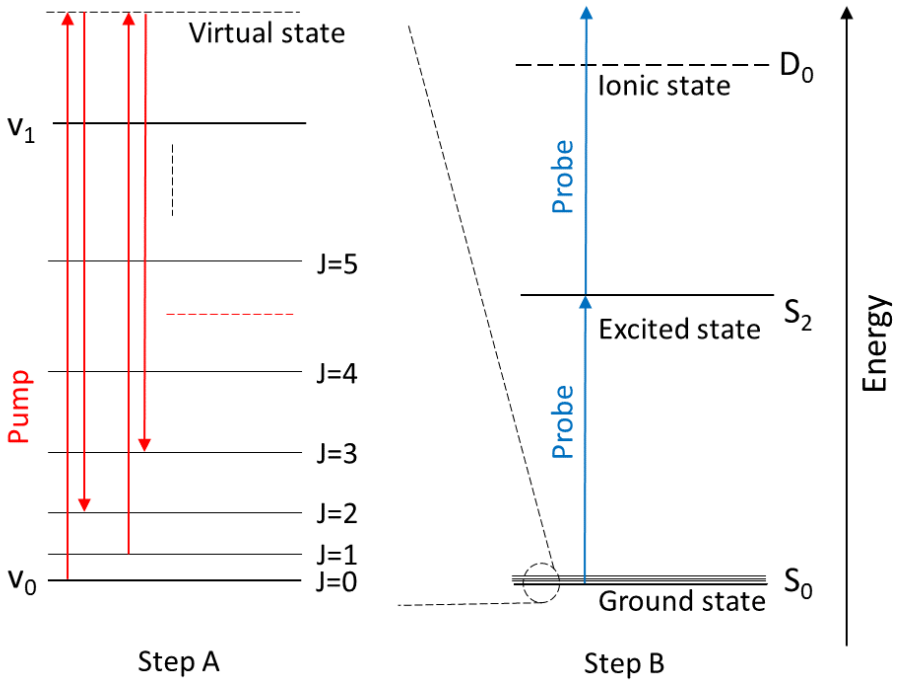

Figure 7. Energy diagram of the pump-probe process for BD in CRASY. (Step A) Coherent rotational Raman excitation by an alignment beam with 800 nm wavelength creates a rotational wave packet in the ground state. (Step B) A subsequent probe beam with 200 nm wavelength generates transitions from the ground state to the ionic state by femtosecond two-photon ionization.

Isotopic substitution is a powerful method to collect structural data in terms of isotopes and their associated dissociative reactions. Molecular structure can be extracted from isotopic substitution using the Kraitchman [7] method. Synthesis of isotopically labelled compounds, however, is expensive and time-consuming. The mass-CRASY experiment couples the ground state rotational structure with ion mass. This allows the identification of naturally occurring isotopologues by assigning their corresponding signals at their respective mass-to-charge ratio. This removes the need for isotopologues synthesis.

Compared to preceding RCS experiments, CRASY provides several improvements: (1) Mass correlation [13] of the rotational spectrum for each species in a molecular beam. (2) High spectroscopic resolution for the rotational Raman spectra. Since CRASY is a time-domain technique, the resolution is limited by the Heisenberg energy uncertainty. Combining opto-mechanical delay stage with electronic delays extended the delay range up to the microsecond range and enhanced the resolution up to a single MHz [11]. (3) Highly accurate spectroscopic frequencies. Absolute frequencies were obtained by directly referencing the oscillation repetition rate to a GPS-stabilized external clock [11].

Halonen et al.[14] obtained high-resolution rotational constants for jet-cooled trans-1,3-butadiene in rotationally resolved IR spectra and investigated the C-H stretching region. They presented a highly-accurate ground vibrational state rotational constants for the main BD isotope. In the same year, Craig et al. [15,16,17,18] interrogated the gas-phase IR and liquid-phase Raman spectrum for 1-^{13}C-BD, completing the analysis of its rotational structure. BD has been analyzed by our group [19] and CRASY revealed the atomic scrambling in the ionic states of BD. In this work, we show correlated data for butadiene isotopologues by means of mass-selective high-resolution rotational spectroscopy.

2. Experimental part

Vaporized butadiene was carried by *10* to *20 bar* pressure Helium gas at the room temperature. A mixture of Butadiene and Helium gas with the ratio of *1:100* were released through a pulsed valve (*Evan Lavie, E.L-7-4-2007-HRR*, *150 μm* nozzle, operating at *500 Hz* and *80 ℃*). The expanding molecular beam was skimmed and arrived in *a Wiley – McLaren* type mass spectrometer (vacuum pressure « 10^{-6} *mbar*) after passing the interaction region (vacuum pressure < 10^{-4} *mbar*). A collimation angle of 0.10^{o} was calculated for the skimmed beam, based on the *1 mm* skimmer that was positioned at *280 mm* distance from the pulsed valve. The mass spectrometer analyzed the masses of photo-ionized cations.

A single femtosecond (*fs*) laser oscillator (*Coherent, Vitara-T*, *80 MHz* repetition rate) generated amplified *fs* laser pulses with a central wavelength of *796 nm*. The laser pulses were split into two parts, alignment and probe pulses, synchronized with electronic timing units (Coherent SDG Elite) and going into regenerative amplifiers (*Coherent, Libra USP-1k-HE-200*, *1 KHz* repetition rate). The alignment pulse was compressed to *150 ~ 1500* fs duration and attenuated to *50 ~ 150 μJ* energy. The ionization pulse was compressed to *45 fs* duration and attenuated to *0.5 μJ* by non-linear BBO crystals. The two pulses with identical linear polarization, were focused with a spherical mirror with *75cm* focal length into the interaction region.

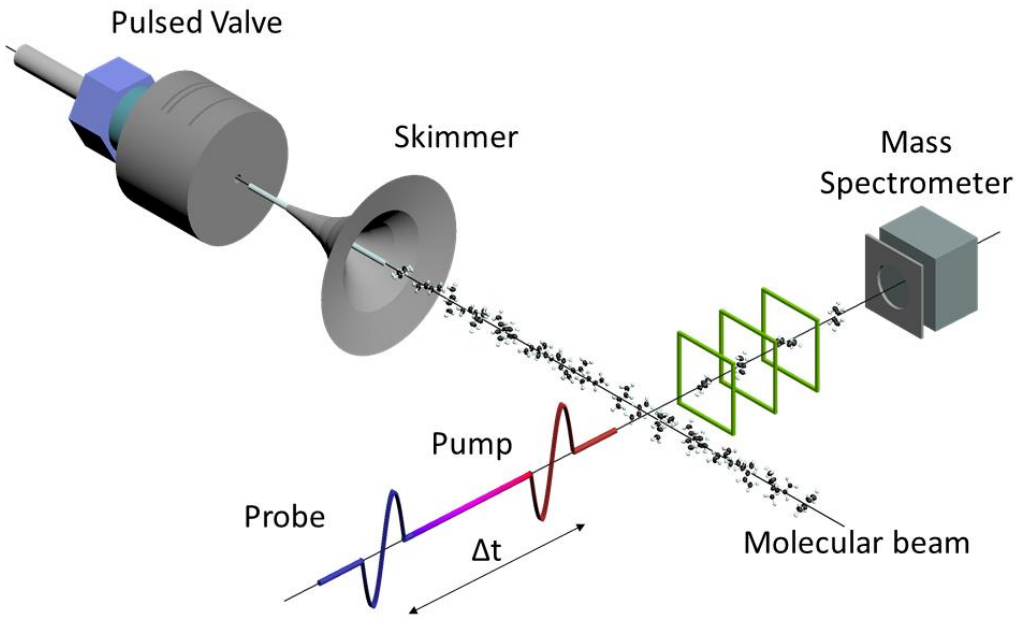

Figure 8. Experimental scheme. A BD molecular beam was expanded from the pulsed valve and passed through the skimmer. Subsequently, the molecular beam interacted with an alignment laser pulse (red) exciting coherent rotational motion. After a time delay of Δt, probe laser pulse (blue) ionizes BD molecules. Formed positive charges move towards the mass detector.

The time delay between the two pulses was controlled by selecting oscillator pulses going into the regenerative amplifiers and by an opto-mechanical delay stage. Oscillator pulses were selected separately for the alignment and ionization amplifiers. Both amplifiers received the selected pulses from the same frequency stable initial oscillator. Those allowed to add discrete delay of $\Delta t = 1/(80\ \text{MHz}) = 12.5\ ns$ with negligible timing-jitter. A frequency counter (*Aim-TTITF930*) measured the oscillator repetition rate against a cheap GPS-stabilized clock (*Leo Bodnar GPSDO*) with a relative accuracy $\Delta v/v < 10^{-8}$. An Allan deviation of $<10^{-10}$ confirmed a stable oscillator repetition rate. The alignment laser pulse was passed through a *30 cm* opto-mechanical delay stage (*Physik Instrumente, MD-531*) with a 100 nm internal encoder. The pathway was folded 16-fold over the stage to acquire *4.8 m (16 ns*) adjustable delays with femtosecond step size (≥ *5 fs*).

For large time delay of the two pulses, a motorized mirror mount modified the position of the alignment laser on the molecular beam to correct for the velocity of the molecular beam of *1100 m/s*. A slight deviation from right angle $(91.6\pm0.4)^{o}$ between the molecular beam and two laser beams induced a small Doppler shift of $(1.0\pm0.26)\cdot10^{-7}$. Doppler broadening was negligible on account of the small collimation angle of the skimmed molecular beam.

A chopper wheel (*Thorlabs MC2000*) was used to alternatingly detect alignment-ionization signal and reference signal. The temporal signal modulations from each mass channel were Fourier transformed to gain rotational Raman spectra.

The laboratory environment temperature and humidity was controlled as *(20±0.5)℃* and *(40±10) %RH*. We used the *NIST shop-floor equation* to calculate the air refractive index with an accuracy under 10^{-7} during the measurement. The delay stage positions were calibrated by measuring cross correlation signals that were displaced by a oscillator pulse jump (*12.5 ns*) and in regard to a temperature insensitive optical encoder (*Sony Laserscale BL57-RE*, thermal expansion coefficient of *0.7·10-6 m/(m·K)).*

3. Results and Discussion

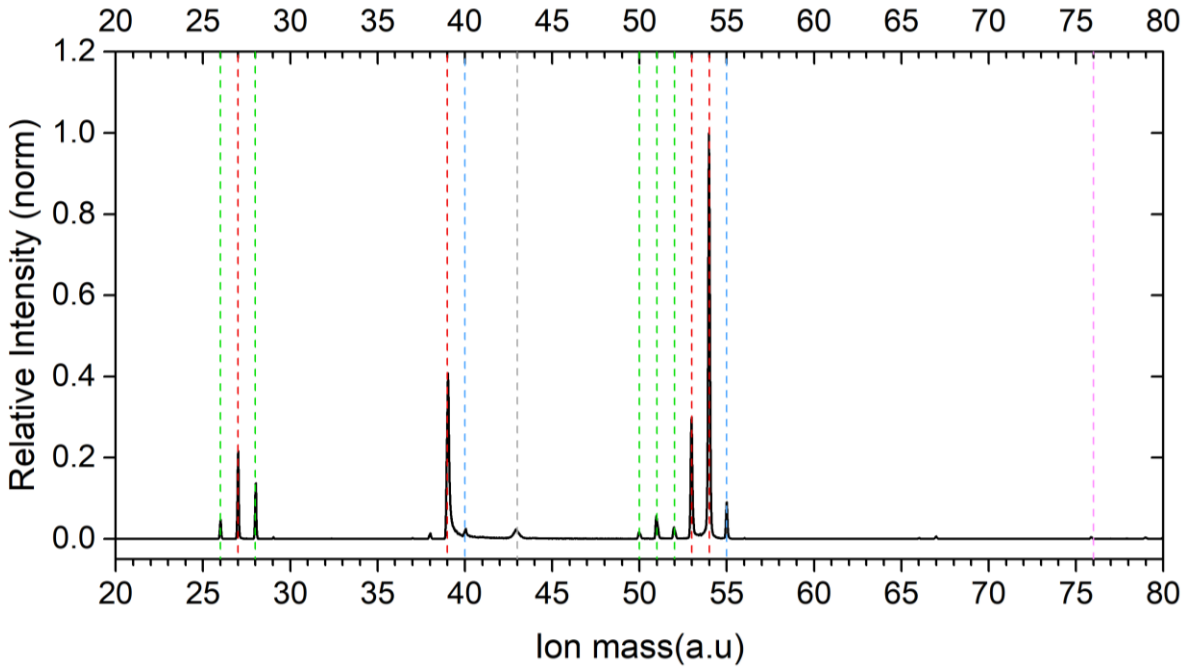

Figure 9. REMPI Mass spectrum of BD and its fragmentation.

The mass spectrum of BD is shown in Figure 9 and its resolution is about 560 (resolution in *m/ΔM*) at *55 u* with a FWHM of *0.09874 (ΔM)*. The fragmentation products of the REMPI process can be tracked along the ion mass axis. The mass peak at *54 u* is the cation of BD *($C_4H_6^+$)* and is assigned to be the base peak. The parent BD ion is formed by UV multi-photon ionization. In this spectrum, the dominant fragment ions observed are $C_4H_5^+$(-*H* loss) at *53 u*, $C_3H_3^+$(-CH_3 loss) at *39 u* and $C_2H_3^+$(-C_2H_3 loss) at *27 u.* The mass signal *55 u* and *40 u* originate from ^{13}C-isotopes of the mass *54 u* and *39 u* species, respectively. Minor fragment ions are $C_2H_2^+$(- C_2H_4 loss) at *26 u,* $C_2H_4^+$(- C_2H_2 loss) at *28 u,* $C_4H_2^+$(- H_4 loss) at *50 u,* $C_4H_3^+$(- H_3 loss) at *51 u*, and $C_4H_4^+$(- H_2 loss) at *52 u*. [4] Their small relative signal amplitudes are due to their high ionization energy as compared to the energy of the REMPI process. Two-photon REMPI of BD with photons of *200 nm* (by forth harmonic generation of 800 nm laser beam) introduces *12.4 eV* of energy into the molecules. Other fragmentation channels with higher ionization energy are beyond the range of this experiment. Apart from butadiene signals, there is a signal of carbon disulfide at *76 u*, which we used as our calibration signal. It has a relative intensity of *0.55 %* compared to the base peak.

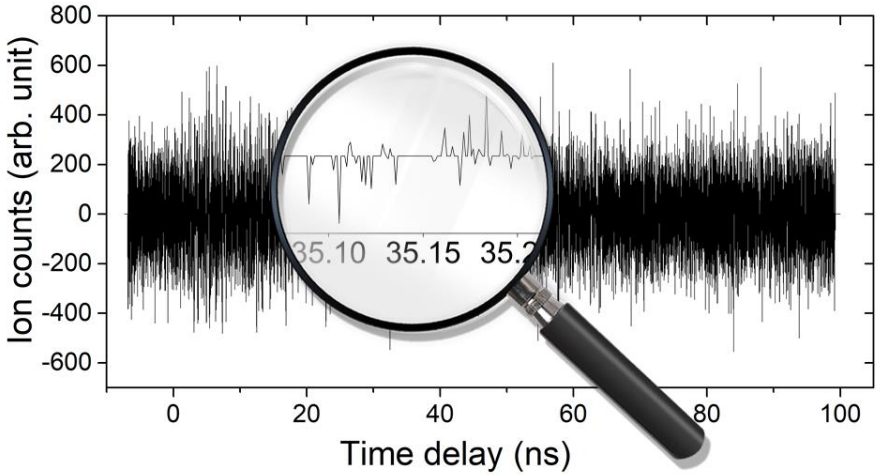

Figure 10. Alignment-ionization time trace for all BD mass channels, including fragments and isotopologues.

Mass spectra were measured at *1 ps* steps over a time delay of *100 ns* (equivalent to a *30 m* mechanical delay). The signals were obtained by impulsive rotational Raman excitation of a coherent rotational wave packet and temporal evolution of subsequent resonant two-photon ionization signals. Each mass signal is modulated by the rotational motion of the molecules in the time domain. Therefore, a corresponding alignment-ionization time trace was obtained for each mass signal in the mass spectrum. Figure 10 shows the summation of the time-resolved mass signals of all mass channels. This measurement of mass spectra over a large alignment-ionization time delay range would generate a huge data set. Nyquist sampling is required to recover a frequency signal, (i.e. *1 ps* sampling to recover frequencies $\leq$ *500 GHz*). A better frequency resolution requires a longer sampling time. To simultaneously obtain a large frequency range (= small sampling step size) and a high resolution (= long sampled delay range) would result in a tremendous experimental cost in terms of time. The experiment may take days even weeks. Hence, random sparse sampling was performed to expedite long measurements. Sparse sampling basically abolishes the requirement of measuring all Nyquist points to recover a signal. Less data points with a random sparsity were measured to build the signal. This, on the other hand, introduces a random noise, resulting in a lower signal-to-noise ratio. The signal noise in the time-domain is converted by Fourier transformation to baseline noise in the frequency spectrum. The sampling ratio in our experiment is *8.79 %*.

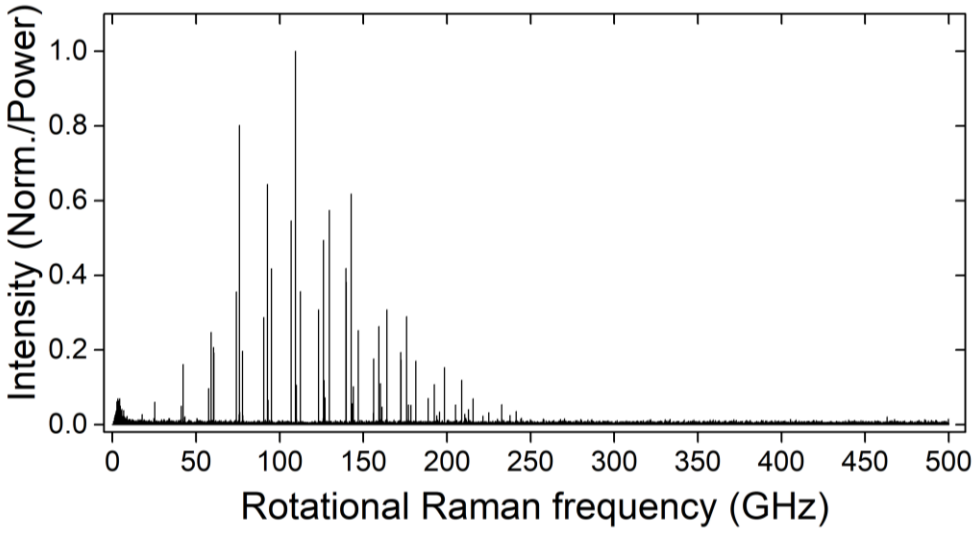

Figure 11. Fourier transformed rotational Raman spectrum from trace in Figure 2.

The rotational Raman spectrum contains information on the rotational transition frequencies and the molecular moments of inertia. To obtain spectra, time domain signals of each mass channel in Figure 2 were Fourier transformed into frequency domain signals as shown in Figure 11. The rotational Raman frequency range in our experiment is *500 GHz* (corresponding to the Nyquist theorem with a temporal step size of *1 ps*). The resolution of each spectral line is approximately *10 MHz full-width-half-maximum (FWHM)*, close to the Fourier limit for the scanned delay range of *107400 ps*. Each peak indicates a rotational Raman transition from one rotational state to another. For the *54 u* mass channel, the rotational transitions are shown in Figure 12. We observe predominantly signals for the *S-branches (ΔJ= +2)* with high amplitudes and only weak signals for the *R-branches (ΔJ= +1)*.

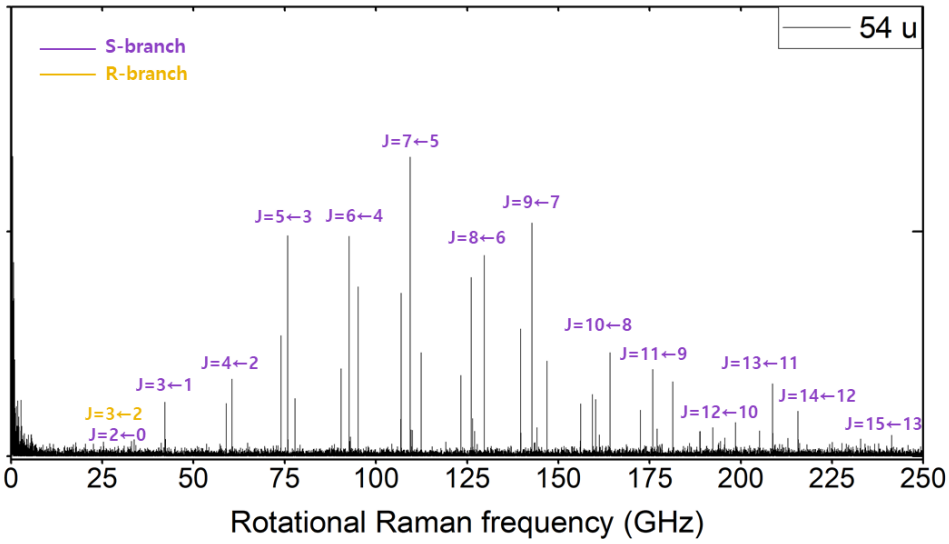

Figure 12. The rotational transitions that in the rotational Raman spectrum of the 54 u mass channel. Red transitions indicate S branches (ΔJ= +2) and green transition indicates the R branches (ΔJ= +1).

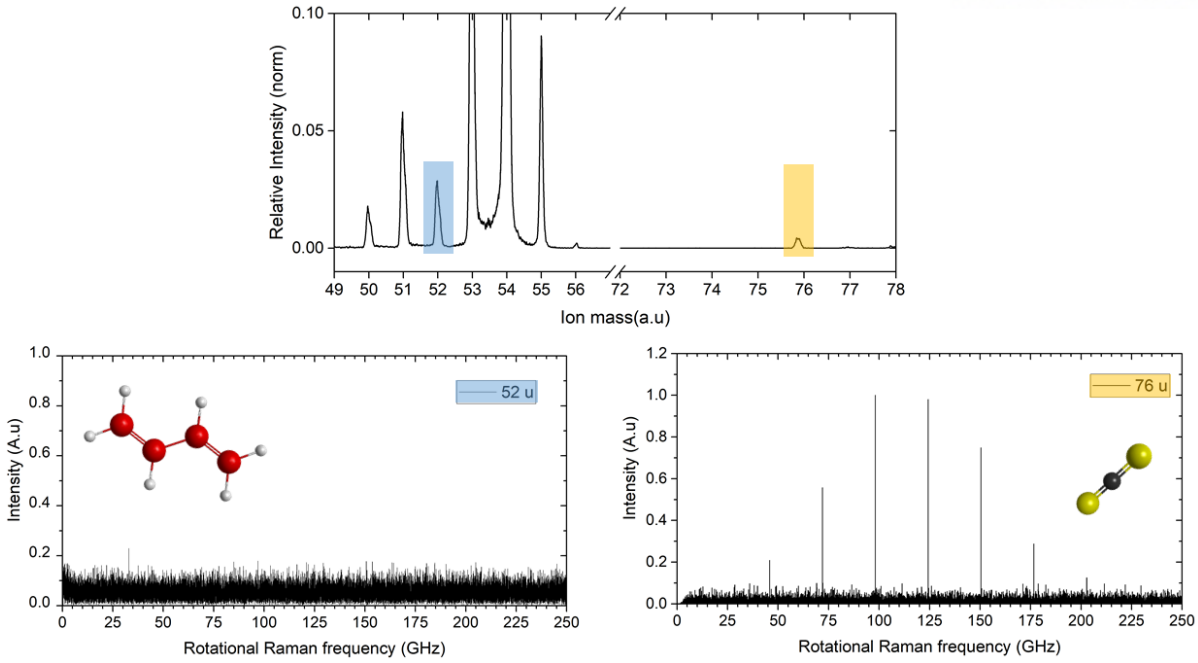

Figure 13. The comparison of mass channel 52 u (BD fragment) and 76 u (main CS_2 isotope).

Now we look closer at one of the smallest peaks in the mass spectrum in Figure 13. We expect the rotational Raman spectrum of the *52 u* mass channel (*0.55%* of the base peak) to have a signal comparable to the noise signal. However, the mass signal in *76 u* (*0.33 %* of the base peak) with a smaller ion counts intensity shows a high signal-to-noise ratio. The reason is that CS_2 molecules have a perfectly symmetric linear molecular structure as oppose to the near-prolate structure of BD. CS_2 therefore has a higher anisotropic polarizability and its rotational Raman excitation is more efficient. Its linear structure leads to a higher degree of alignment that creates larger signal peaks. In addition, CS_2 has less spectral lines due to the nuclear spin statistics whereas BD has much more spectral lines. The spectral lines of BD are spread all over the spectrum, and this causes higher signal-to-noise ratio,. This CS_2 signal in mass channel 76 u was used as our calibration signal.

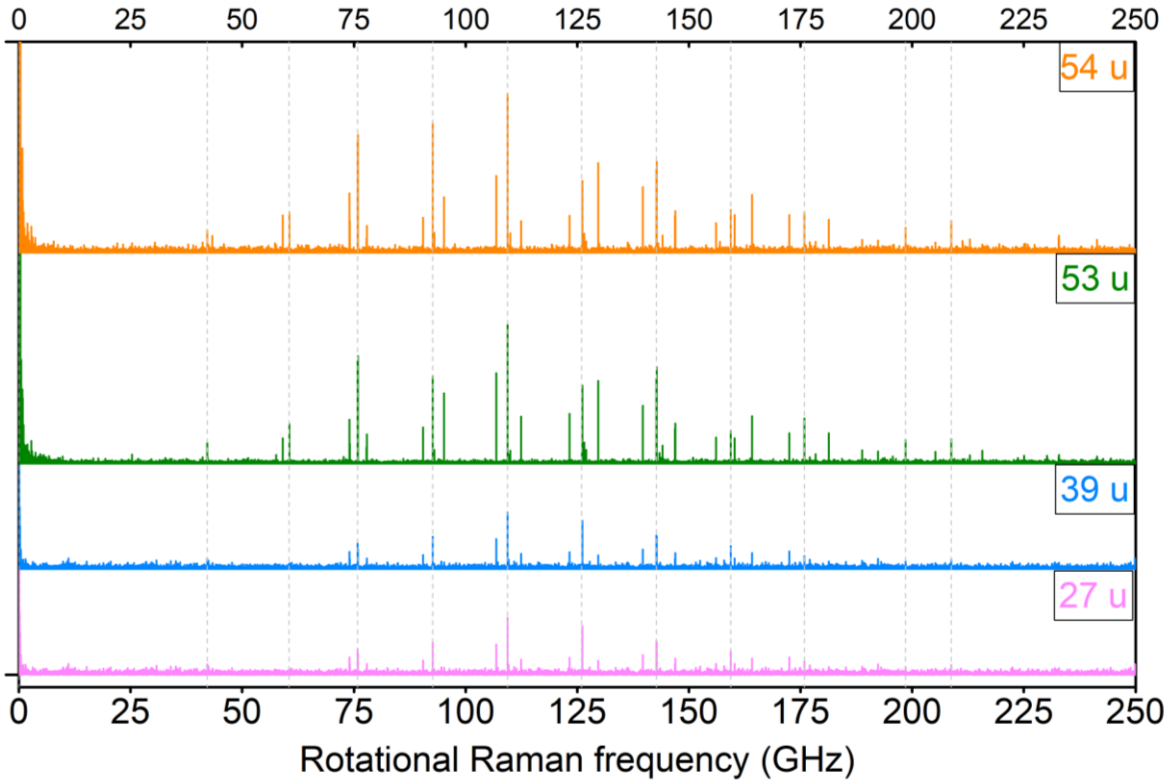

Figure 14. Mass-CRASY data of butadiene and its major fragments. The cations of $C_4H_5^+$(-*H* loss) at *53 u*, $C_3H_3^+$(-CH_3 loss) at *39 u* and $C_2H_3^+$(-C_2H_3 loss) at *27 u* show identical rotational spectra, they therefore belong to the same BD precursor.

The mass-CRASY data of major fragments of BD is shown in Figure 14. The parent molecular ion $C_4H_6^+$, butadienyl cation $C_4H_5^+$ and cyclopropyl $C_3H_3^+$ and $C_2H_3^+$ were observed at mass *54 u, 53 u, 39 u*, and *27 u*, respectively. As clearly seen, all three cations showed identical rotational Raman signals, indicating that they are formed from the same parent precursor of butadiene. The reason behind this is the following: The pump-probe experiment of CRASY is performed in a Wiley-McLaren mass spectrometer's interaction region. Therefore, parent BD molecules are excited and probed into the BD cation before any fragmentation occurs. The measured (probed) rotational Raman spectra shows the rotational Raman frequencies that corresponds to the quantized rotational motion of the BD neutral. The dissociation later generates different fragment ions to be detected by the mass spectrometer.

Fragmentation of BD in the ionic state occurs on a time scale comparable to that of ionic acceleration (microseconds) in the TOF spectrometer. Some fragment signals therefore showed a tail towards higher mass channels. The elongated tails appeared at ion masses of *40 u* and *53.5 u* [Appendix B] in Figure 9 and are from the slow fragments corresponding to *39 u* and *54 u*, respectively. Figure 15 illustrates the mass channel *40 u*, where both the heavy isotope- $C_3H_3^+$ *(40 u)* fragment and the slow fragmentation product $C_3H_3^+$ *(39 u)* are present. The overlap integrals in the zoomed boxes shows the agreement of Raman transition frequencies of mass channels *39 u* and *40 u*. However, signals due to the light isotope are clearly recognizable yet heavy ones are not. The first reason is that there are two isotopologues of cyclopropenyl cation which are *1* – ^{13}C and *2* – ^{13}C Hence, that divides the signal by a factor of 2. The second reason is due to the symmetry of the light isotope of BD versus the broken symmetry of the heavy-carbon substituted BD. The broken symmetry divides the signal by another factor. With the mentioned reasonings, the signal in *40 u* is split into many distinct lines which vanish into the noise. The current CRASY experiment cannot resolve the peaks of heavy of BD isotope in mass channel *40 u*.

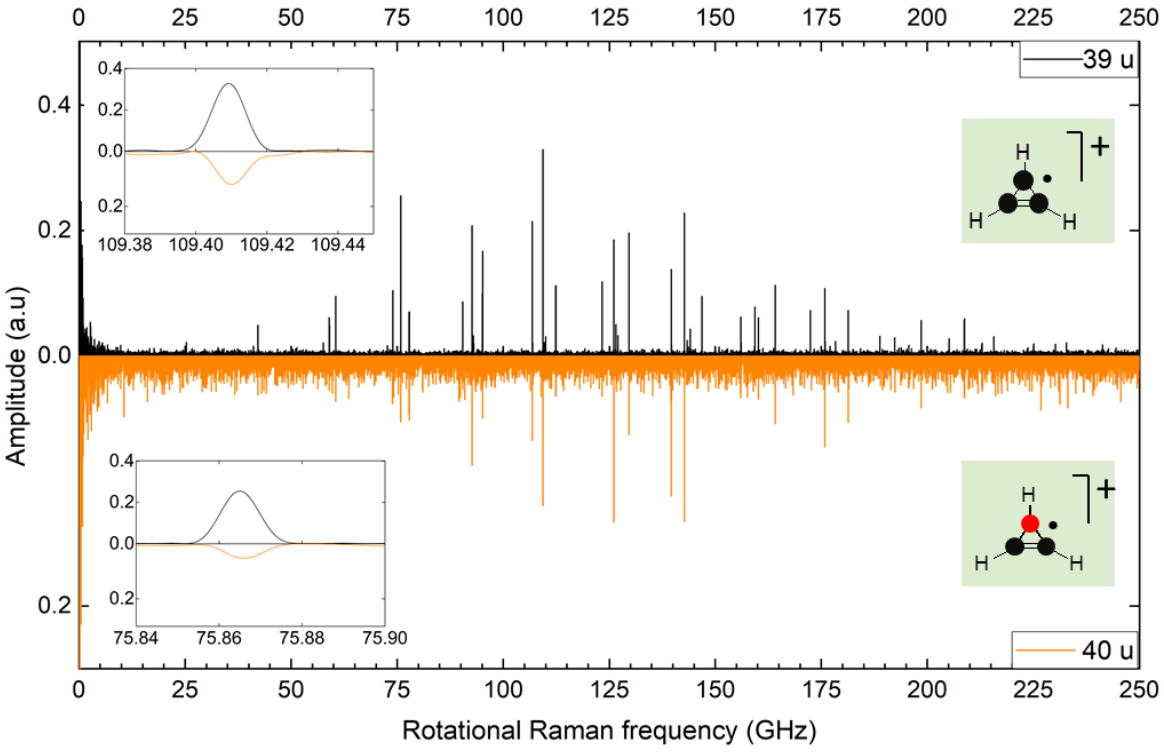

Figure 15. Comparison of Rotational Raman spectra of ion mass channels 39 u (black) and 40 u (orange). The signals in mass channel 40 u are due to the cyclopropenyl cation $C_3H_3^+$ containing a heavy carbon isotope. The signals in mass channel 39 u are only due to the cyclopropenyl cation $C_3H_3^+$. The zoomed insets illustrate the overlapping integral of the signals for both ion mass channels.

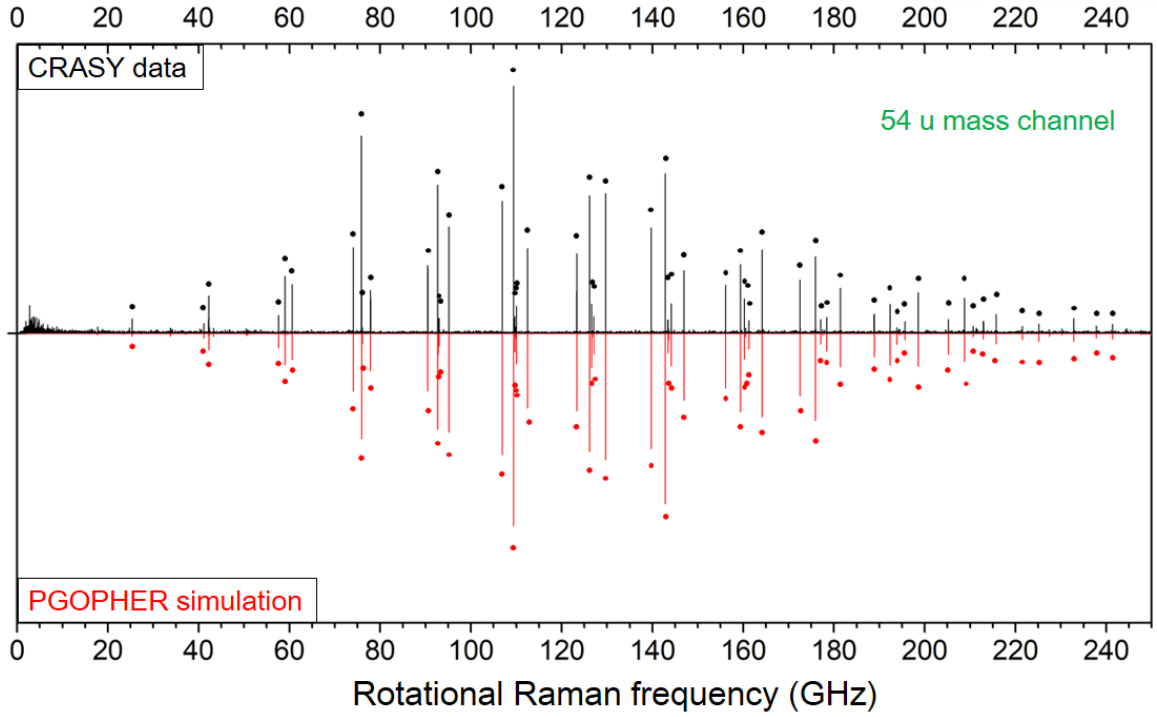

Figure 16. Experimental (top) and simulated (bottom) rotational Raman spectrum of BD. The top spectrum shows the main isotope of butadiene. The dots represent the peak assignment for the fitting of our data.

An analysis of Raman rotational spectra was carried out using PGOPHER. [20] Spin state statistics were considered to obtain the correct amplitude ratios in the PGOPHER simulation. By means of Fermi statistics, the population statistics of even to odd states of BD shows the ratio of *28:36*. Rotational constants for the main BD isotopologue were obtained by fitting 59 bands for mass channel 54 u, assigned through a comparison with simulated spectra. The assigned peaks are marked in Figure 16. Rotational constants *A, B, C* and distortion constants D_j, D_{jk}, D_k from the work of Craig [15], were used as starting parameters. We fixed *A*, D_j, D_{jk}, D_k constants and fitted *B, C* constants. Further details on the simulation parameters [*Appendix C*] and band assignment [*Appendix D, Table 3*] for main BD isotope can be found in *Supporting information*. Fitted rotational constants and literature values are summarized in Table 1.

	OUR WORK (MHz)	LITERATURE (MHz)	
	BD**	BD*	BD**
A	fixed	41682.780(117)	41682.658(21)
B	4433.4178(85)	4433.444(23)	4433.505(3)
C	4008.1049(70)	4008.061(23)	4008.042(6)
D_k	fixed	—	0.21939(9)
D_{jk}	fixed	—	0.007323(15)
D_j	fixed	—	0.0008763(12)

Table 1. Measured rotational constants and corresponding literature values for BD. * and ** respectively represent Halonen2004, Craig2008.

Our values for the main BD isotope are in good agreement with the reported literature values of Halonen et al., however there is an approximately 9σ difference with Craig et al. The precision of our result is 1 order of magnitude better than that of [14], which is the most accurate literature data. The rotational constants for *1-^{13}C-BD* agree with the literature [14,18]. The distortion constants could not be refined as compared to the literature values, because only low rotational states (around J'=25) were observed.

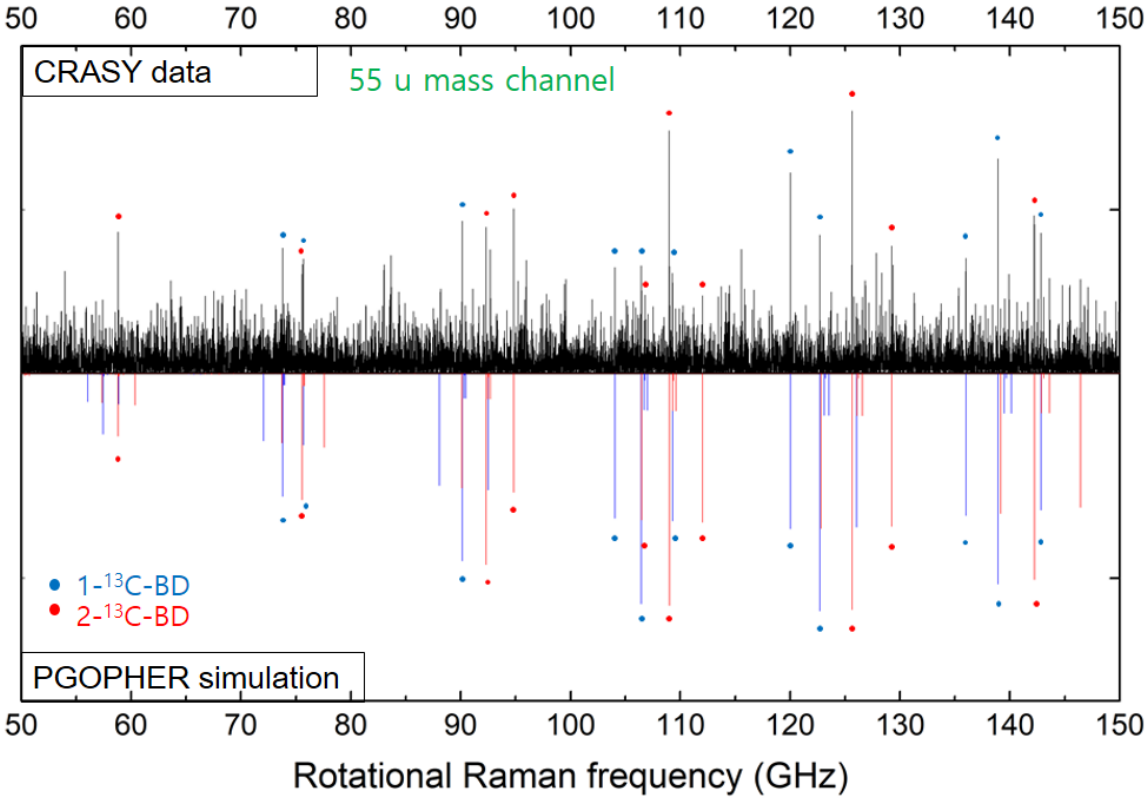

Figure 17. Experimental and simulated data for *1-^{13}C* and *2-^{13}C*. The experimental spectrum (top) is obtained from the ion mass channel 55 u. The PGOPHER simulated spectrum (bottom) shows the heavy-carbon isotopes of BD, which are 1 – ^{13}C-BD (blue) and 2 – ^{13}C-BD (red).

Due to the superposition of five isotope signals of butadiene (*1-^{2}D, 2-^{2}D, 3-^{2}D, 1-^{13}C, 2-^{13}C*) and due to the breaking of symmetry, the mass channel *55 u* showed a more complicated spectrum as compared to the mass channel *54 u*. As the rotational moment of inertia increases with isotopic substitution, the rotational constants decrease and the transition frequencies are shifted toward smaller values. The probability ratio of observing deuterated BD over ^{13}C-substituted BD is *1:64*. Therefore, deuterated isotopes can be neglected in the interpretation of the lines in the spectrum. The spectra in Figure 17, therefore, were assigned to the major isotopes of *1-^{13}C* and *2-^{13}C*. The simulated transition frequencies coincided accurately with the measured rotational Raman signal. However, the band amplitudes of the PGOPHER simulation and the CRASY data differ. The possible reason for this discrepancy is the low signal-to-noise ratio in our data. High-resolution CRASY allowed us to separate the two main *^{13}C*

isotopes of BD and rotational constants for pure *2-^{13}C-BD* are calculated for the first time by CRASY. We assigned 11 bands for *1-^{13}C-BD* [*Appendix D, Table 4*] and 10 bands for *2-^{13}C-BD* [*Appendix D, Table 5*]. The rotational constants were obtained by fitting the mass channel *55 u* spectrum in PGOPHER and listed in Table 2. Due to the low isotope abundance of *^{13}C*, a greater uncertainty appeared for *1-^{13}C-BD* as compared to the main isotope.

	OUR WORK (MHz)		LITERATURE (MHz)	
	1-^{13}C-BD	2-^{13}C-BD	1-^{13}C-BD**	2-^{13}C-BD**
A	fixed	fixed	41634.934(18)	—
B	4306.930(42)	4419.584(93)	4307.067(9)	—
C	3904.083(34)	3991.255(96)	3904.050(9)	—
D_k	fixed	—	0.217652(27)	—
D_{jk}	fixed	—	0.006928(15)	—
D_j	fixed	—	0.0008118(24)	—

Table 2. Measured rotational constants and corresponding literature values for BD. ** respectively represent Craig2004 literature.

4. Conclusion

Butadiene was investigated by a novel spectroscopic method, CRASY, in which rotational Raman excitation, rotational coherence spectroscopy (RCS), resonance enhanced multiphoton ionization (REMPI) and time-of-flight mass spectrometry were combined into a single experiment. CRASY allowed us to observe the mass data of naturally occurring isotopologues and their corresponding rotational signals simultaneously. An analysis of the gas-phase rotational spectrum of 1,3-trans-butadiene (BD) and its most abundant isotopologues of *1-^{13}C-BD* and *2-^{13}C-BD* was performed. The correlated nature of CRASY allowed us to resolve the *BD* isotopes. Opto-mechanical delay stage, sparse sampling and pulse jumping settled CRASY into high resolution spectroscopic regime. This achieved an order of magnitude better precision in rotational constants compared to the established high-resolution experiments. A GPS-stabilized external clock provided a highly accurate rotational constants within our precision, because it removed any systematic error in the experiment. We also revealed the rotational constants of pure *2-^{13}C-BD* for the first time.

5. Acknowledgement

I would like to express my gratitude to my supervisor Professor Thomas Schultz for all his academical guidance and spiritual encourage. He consistently supported me and my work without any hesitation. I also acknowledge the great contribution of Dr. Christian Schröter and my colleagues Jong-Chan Lee and In Heo on experimental set-up and data analysis process.

6. Supplementary Information

APPENDIX A

Rotational Raman spectra of all BD fragments

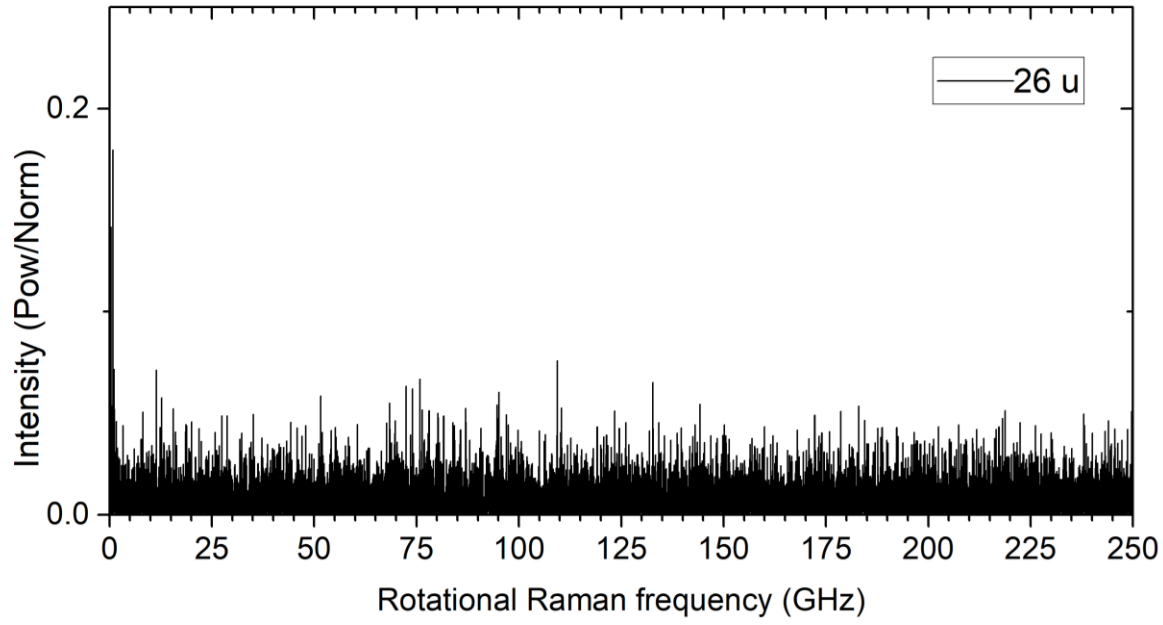

Figure 18. Rotational Raman spectrum of 26 u mass channel.

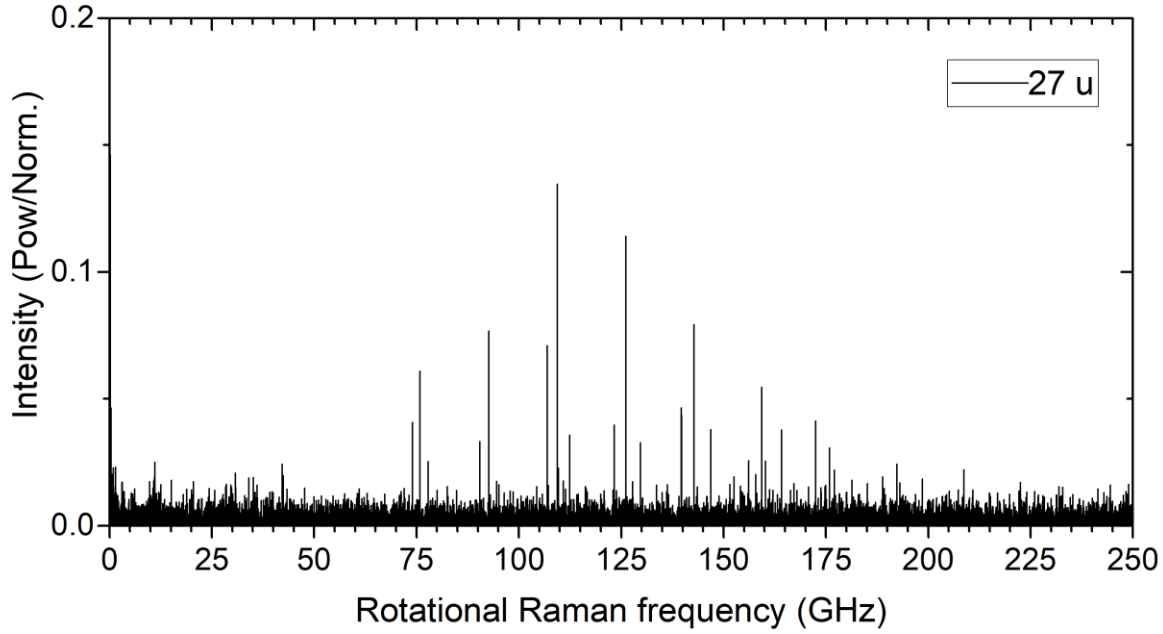

Figure 19. Rotational Raman spectrum of 27 u mass channel.

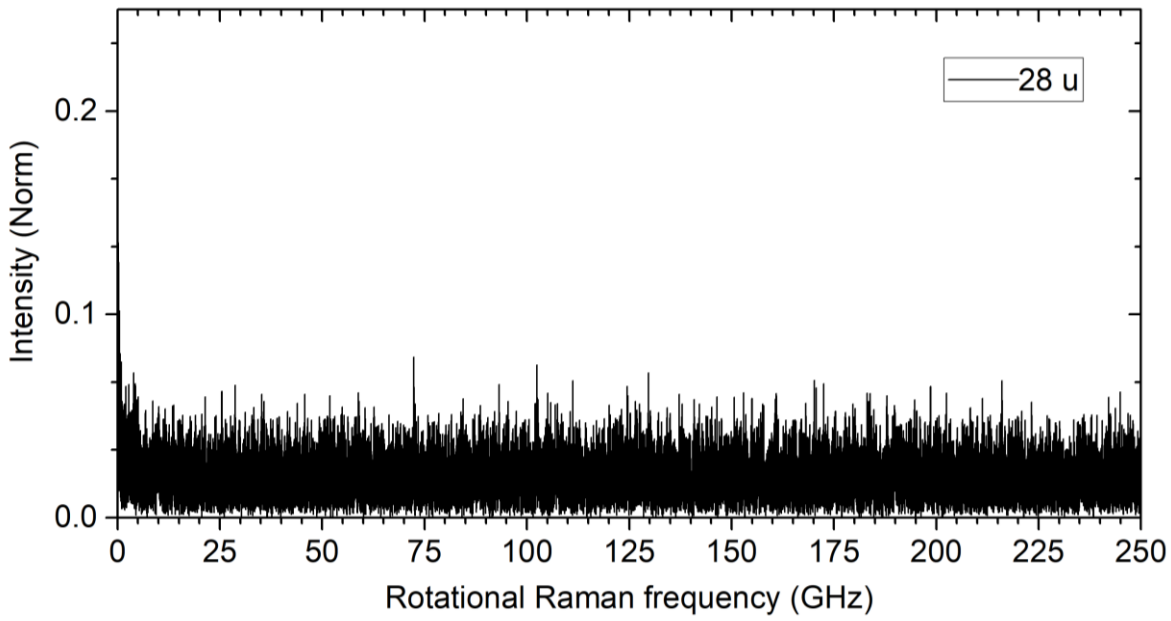

Figure 20. Rotational Raman spectrum of 28 u mass channel.

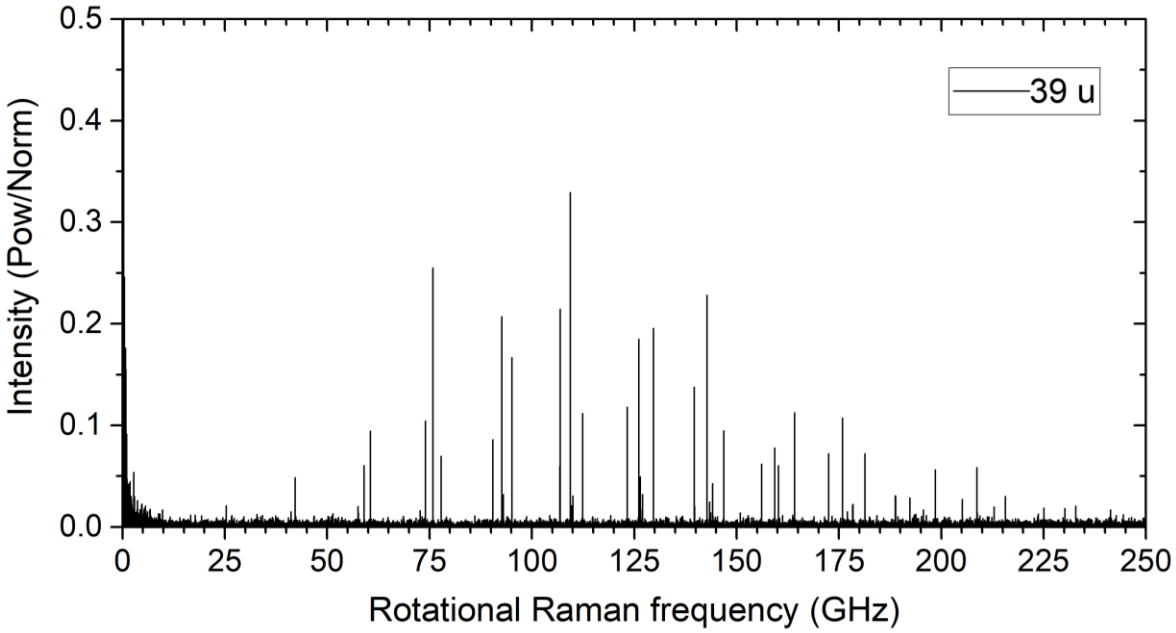

Figure 21. Rotational Raman spectrum of 39 u mass channel.

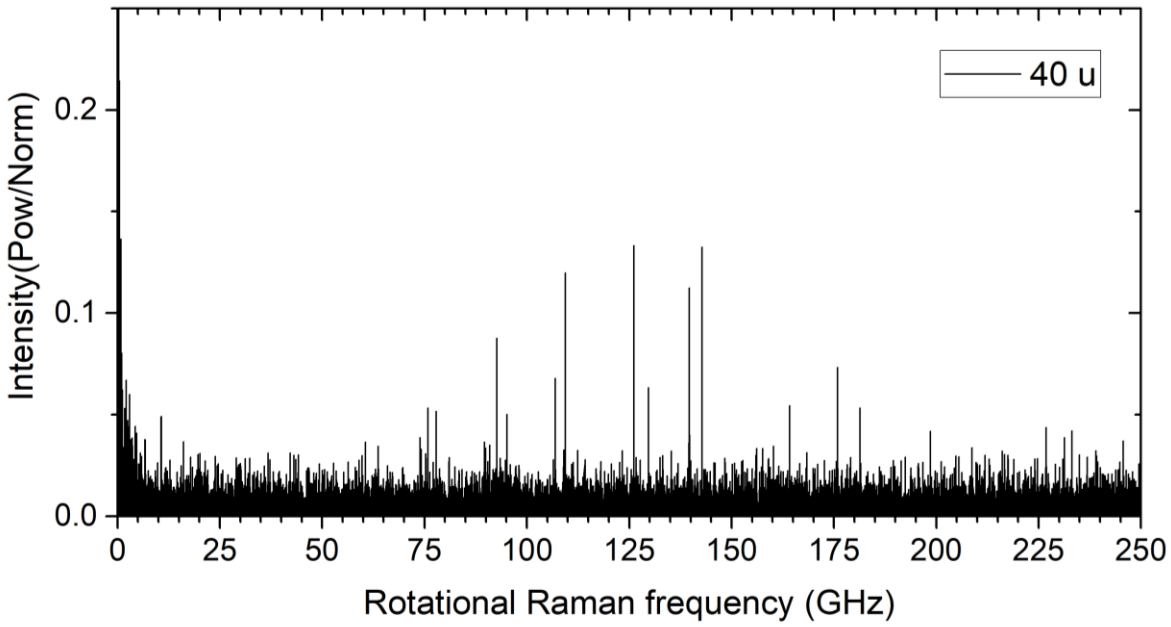

Figure 22. Rotational Raman spectrum of 40 u mass channel.

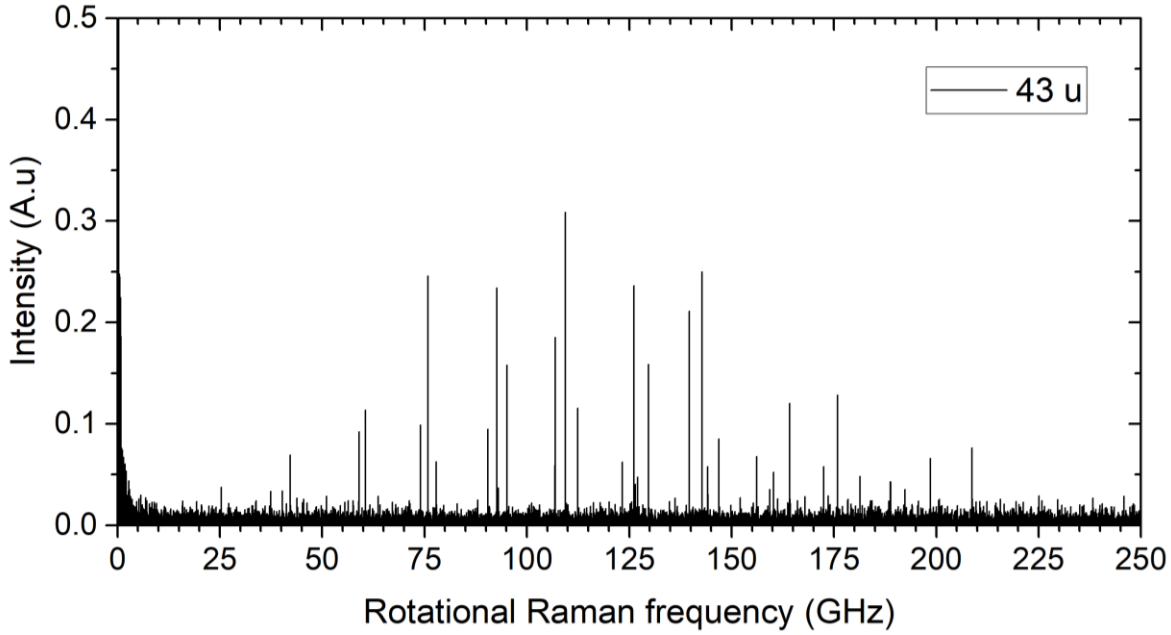

Figure 23. Rotational Raman spectrum of 43 u mass channel.

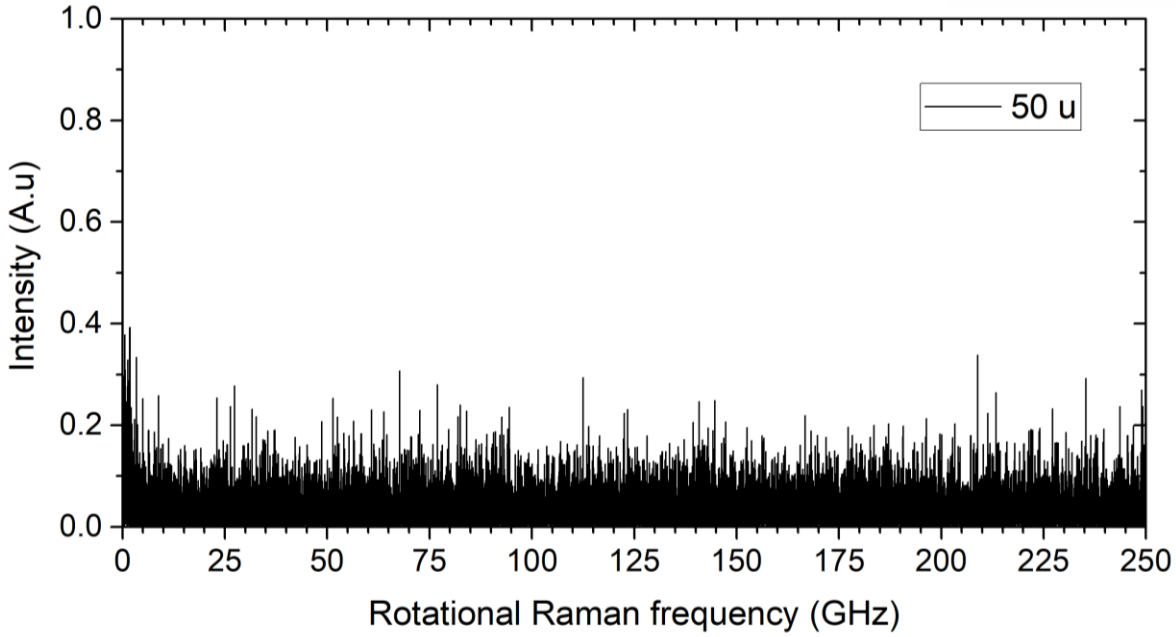

Figure 24. Rotational Raman spectrum of 50 u mass channel.

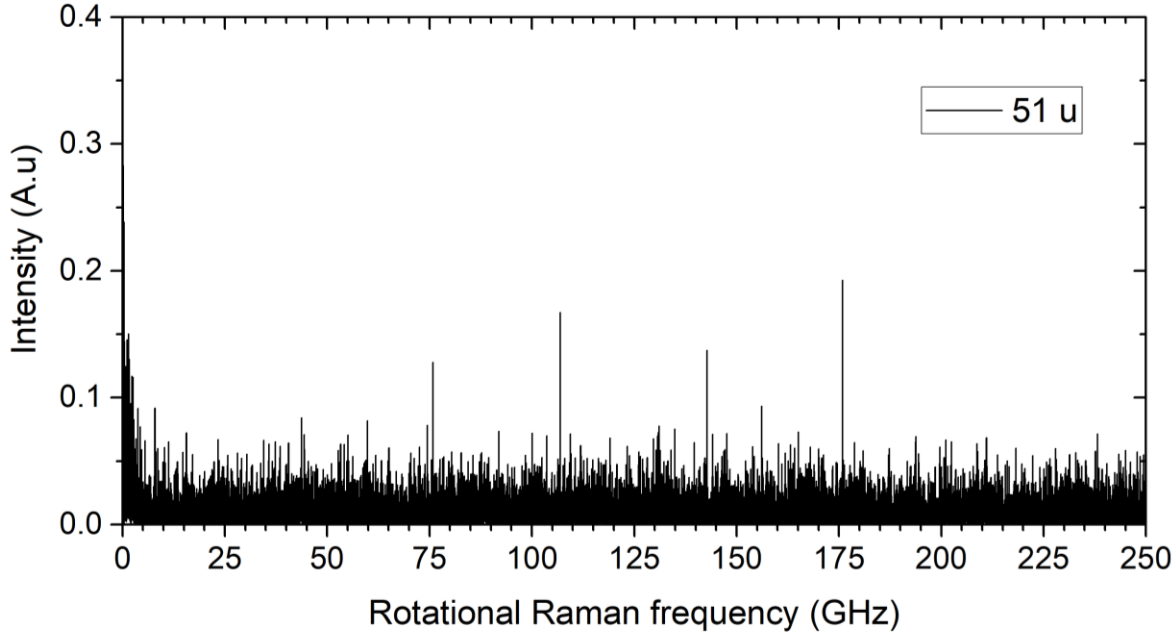

Figure 25. Rotational Raman spectrum of 51 u mass channel.

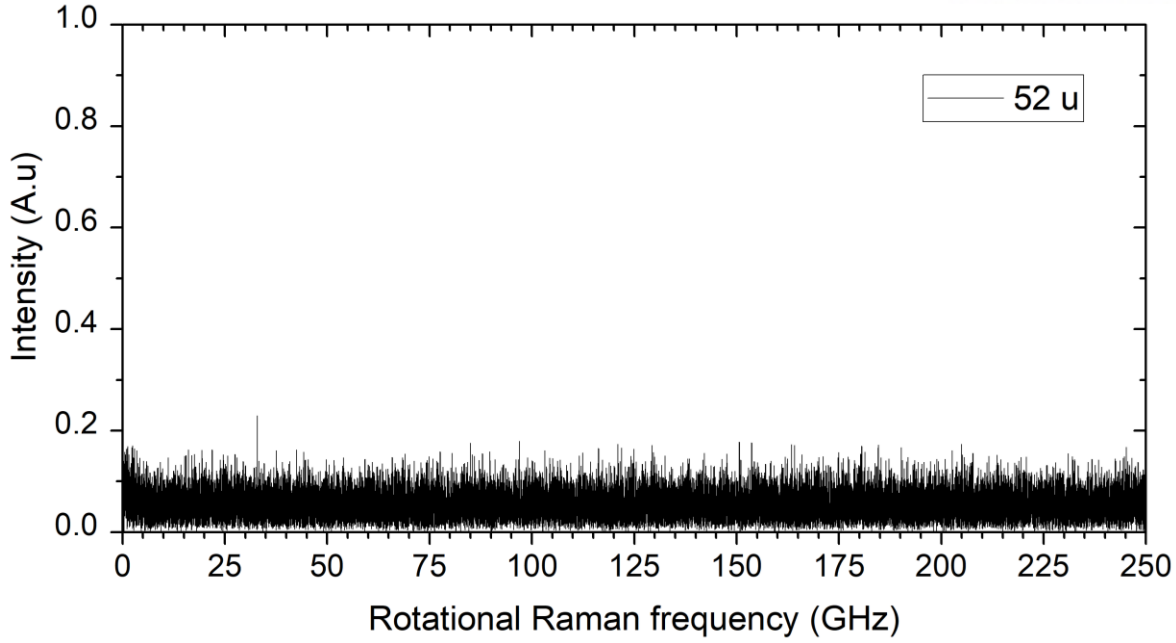

Figure 26. Rotational Raman spectrum of 52 u mass channel.

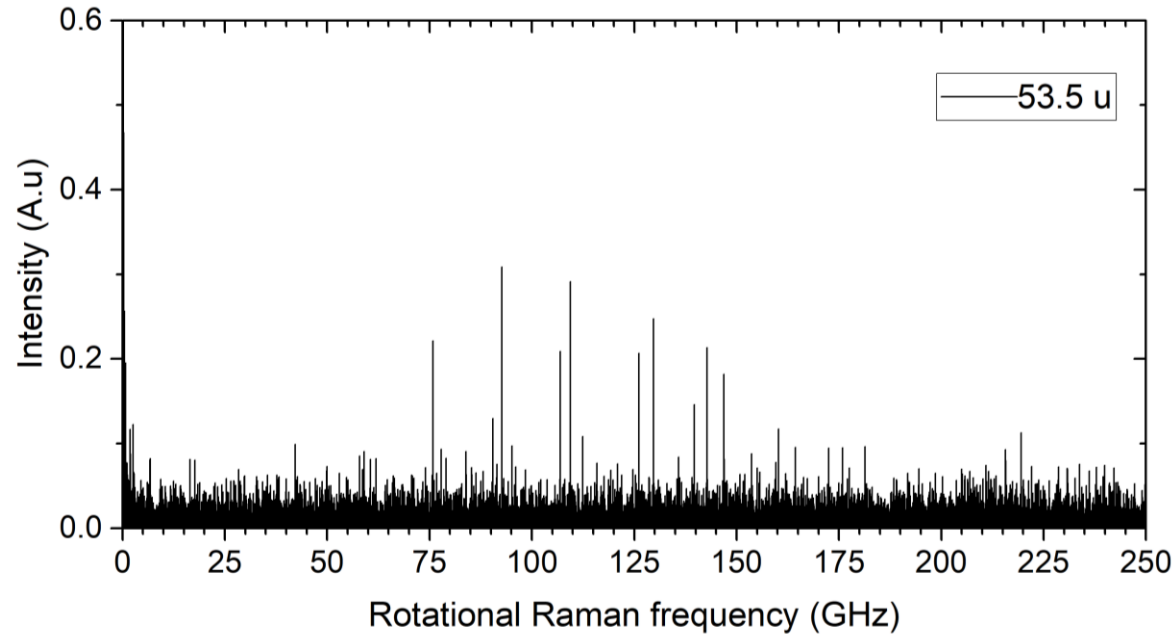

Figure 27. Rotational Raman spectrum of 53.5 u mass channel.

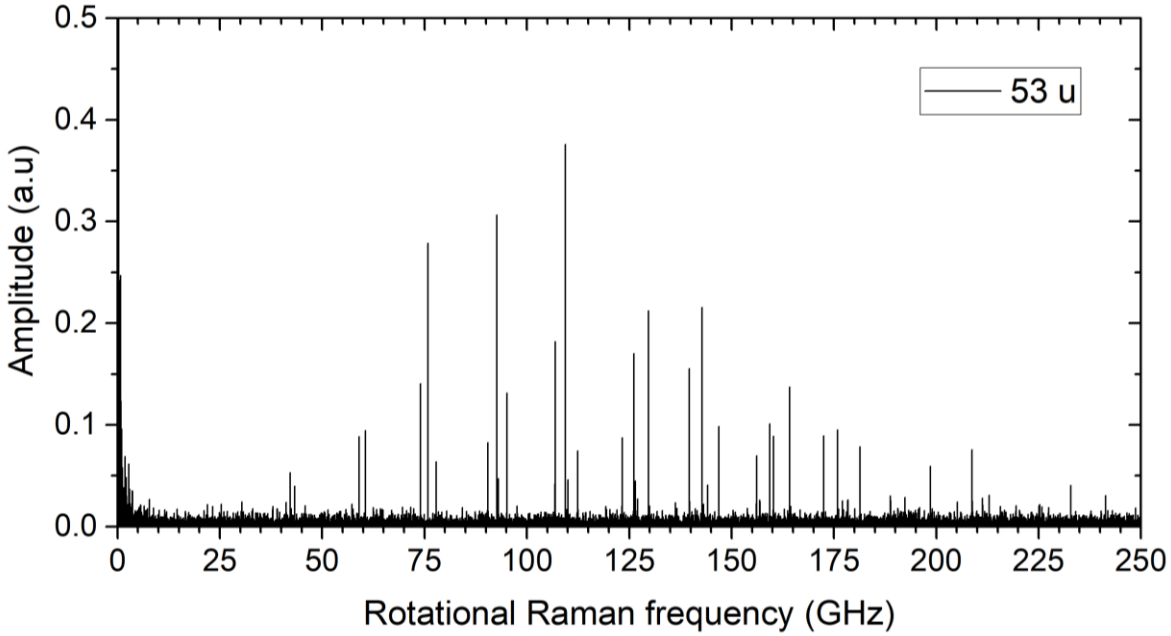

Figure 28. Rotational Raman spectrum of 53 u mass channel.

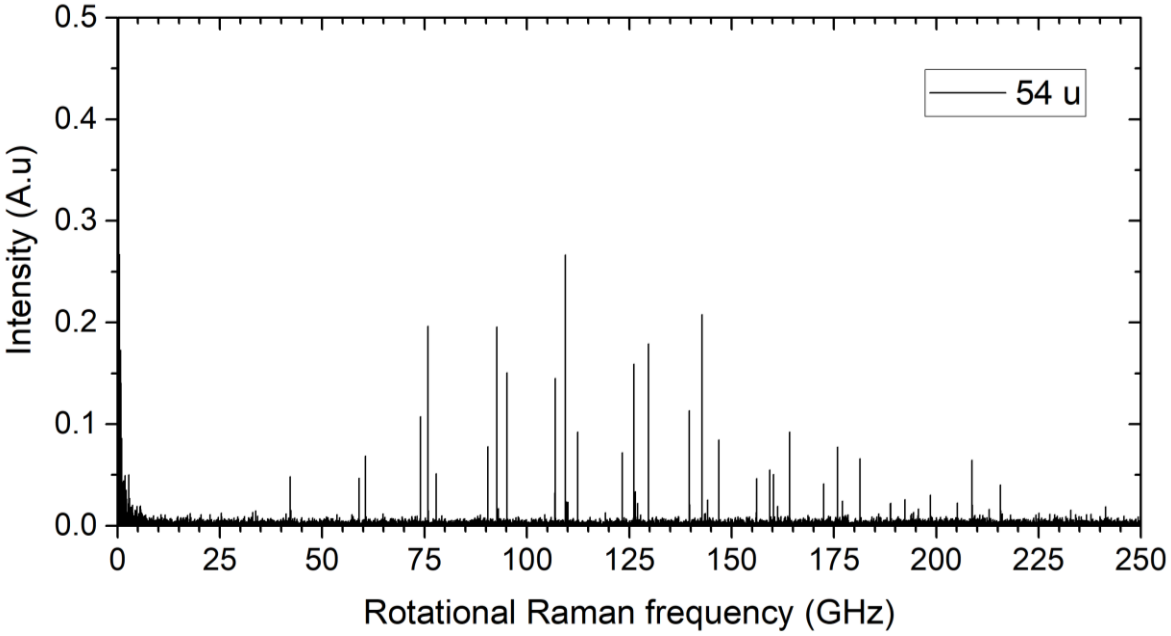

Figure 29. Rotational Raman spectrum of 54 u mass channel.

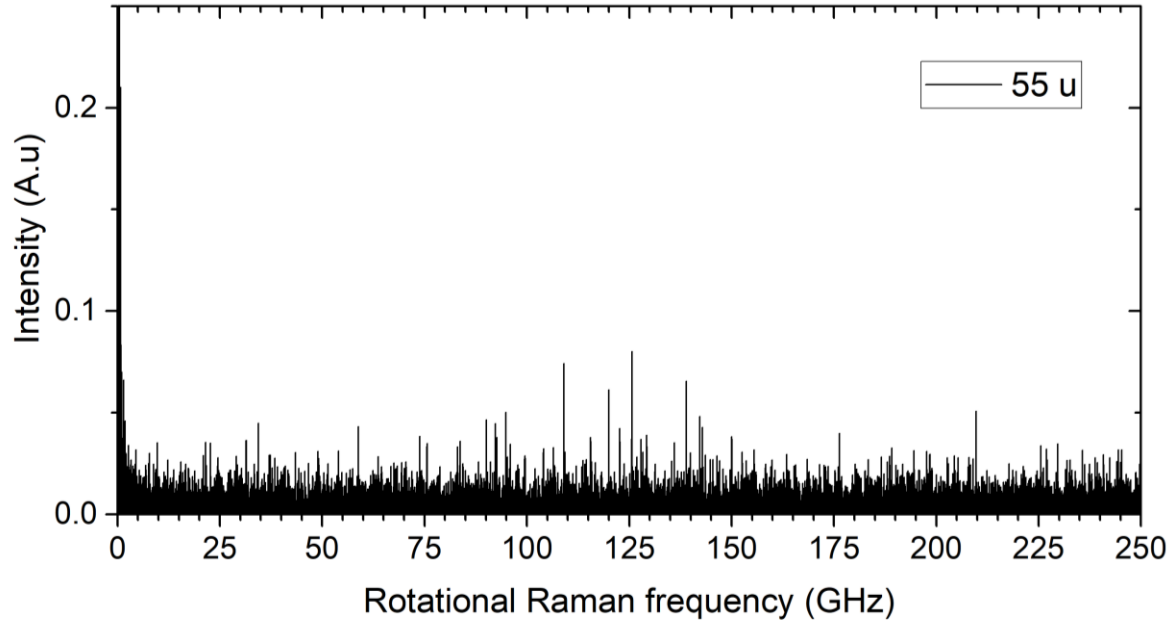

Figure 30. Rotational Raman spectrum of 55 u mass channel.

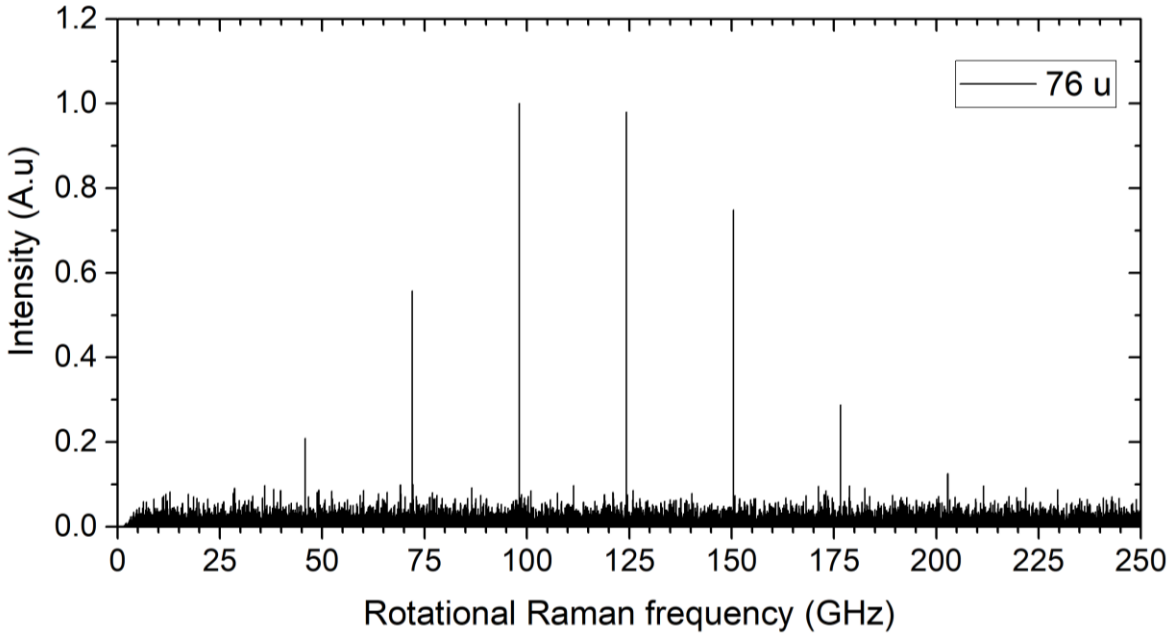

Figure 31. Rotational Raman spectrum of 76 u mass channel. (CS_2)

APPENDIX B

Slow fragmentation

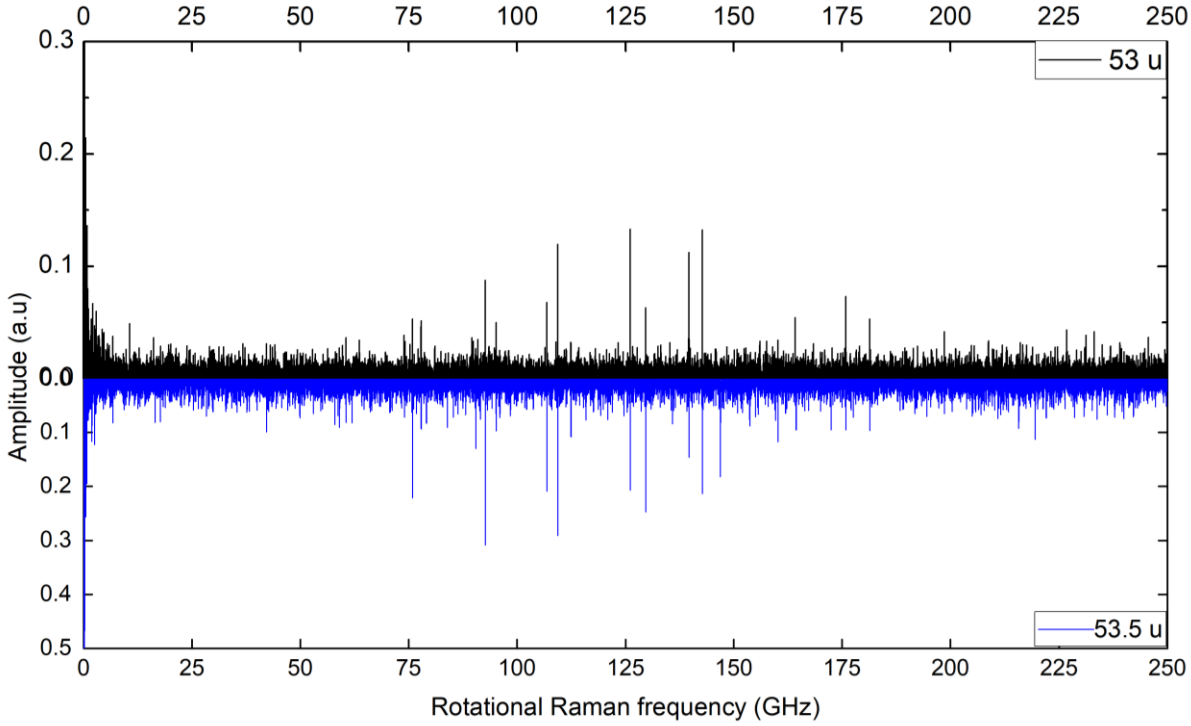

Figure 32. Slow fragmentation channel. Comparison of rotational Raman spectra of ion mass channels 53 u (black) and 53.5 u (blue). The signals in mass channel 53.5 u is due slow fragments of 53 u.

APPENDIX C

PGOPHER simulation

Symmetry is one of the most crucial components on assigning an asymmetric-top molecule in *PROGPHER*. For BD, which is a near-prolate asymmetric top molecule, *the point group, representation*, C_{2z} *axis* and C_{2x} *axis* were set to C_{2h}, *Ir, c* and *a,* respectively. In examination of the symmetry of rotational wavefunction, the notations of *eeWt/eoWt/oeWt/ooWt* are required. These notations define whether the quantum numbers K_a and K_c respectively are *even* or *odd*. In *PGOPHER* simulation, spin state statistics is considered for correction of the amplitude ratios. By means of Fermi statistics, the population statistics of even to odd states of BD shows the ratio of 28:36. Hence *eeWt/eoWt/oeWt/ooWt* respectively are set to *28/36/28/36*. As mentioned before, Gaussian contribution to FWHM is 10 MHz. Since CRASY use rotational Raman excitation to pump to molecules, the transition rank is set to 2. Finally, the rotational and distortion constants are taken from the work of Craig et al as listed in Table 1. We fixed *A,* D_j, D_{jk}, D_k and fitted *B, C* constants throughout *PGOPHER* simulation.

APPENDIX D

The assigned peak list of main BD isotope

J'	Sym'	J''	Sym''	Position	E_{upper}	El_{ower}	Branch (ΔK,ΔJ)	v/J/Ka/Kc (final, initial)
2	E+g	0	E+g	25320.91	25320.91	0	Q,S	v=0 2 0 2 - v=0 0 0 0
3	O-g	1	O-g	42189.38	50630.9	8441.519	Q,S	v=0 3 0 3 - v=0 1 0 1
3	E+g	1	E+g	41142.03	86832.58	45690.55	Q,S	v=0 3 1 3 - v=0 1 1 1
3	E-g	2	E+g	25321.03	200493.4	175172.4	Q,R	v=0 3 2 2 - v=0 2 2 0
4	O-g	2	O-g	57592.41	119740.7	62148.29	Q,S	v=0 4 1 4 - v=0 2 1 2
4	E+g	2	E+g	59039.66	84360.57	25320.91	Q,S	v=0 4 0 4 - v=0 2 0 2
4	E-g	2	E-g	60569.46	123993.7	63424.23	Q,S	v=0 4 1 3 - v=0 2 1 1
5	O+g	3	O+g	77863.73	167248.2	89384.44	Q,S	v=0 5 1 4 - v=0 3 1 2
5	O-g	3	O-g	75864.49	126495.4	50630.9	Q,S	v=0 5 0 5 - v=0 3 0 3
5	O-g	3	O-g	76071.25	276582.8	200511.5	Q,S	v=0 5 2 3 - v=0 3 2 1
5	E+g	3	E+g	74036.44	160869	86832.58	Q,S	v=0 5 1 5 - v=0 3 1 3
6	E+g	4	E+g	92656.74	177017.3	84360.57	Q,S	v=0 6 0 6 - v=0 4 0 4
6	E+g	4	E+g	93030.66	327341.7	234311	Q,S	v=0 6 2 4 - v=0 4 2 2
6	O-g	4	O-g	90472.41	210213.1	119740.7	Q,S	v=0 6 1 6 - v=0 4 1 4
6	O+g	4	O+g	92831.85	327088.6	234256.7	Q,S	v=0 6 2 5 - v=0 4 2 3
6	E-g	4	E-g	95149.37	219143.1	123993.7	Q,S	v=0 6 1 5 - v=0 4 1 3
7	E-g	5	E-g	109694.1	386150.3	276456.1	Q,S	v=0 7 2 6 - v=0 5 2 4
7	O+g	5	O+g	112424.3	279672.5	167248.2	Q,S	v=0 7 1 6 - v=0 5 1 4
7	O+g	5	O+g	109791.3	573576.9	463785.6	Q,S	v=0 7 3 4 - v=0 5 3 2
7	O-g	5	O-g	109409.4	235904.8	126495.4	Q,S	v=0 7 0 7 - v=0 5 0 5
7	O-g	5	O-g	110022.5	386605.3	276582.8	Q,S	v=0 7 2 5 - v=0 5 2 3
7	E+g	5	E+g	106898.7	267767.7	160869	Q,S	v=0 7 1 7 - v=0 5 1 5
7	E+g	5	E+g	109787.8	573572.8	463785	Q,S	v=0 7 3 5 - v=0 5 3 3
8	E+g	6	E+g	126115.9	303133.2	177017.3	Q,S	v=0 8 0 8 - v=0 6 0 6
8	E+g	6	E+g	127052.2	454393.9	327341.7	Q,S	v=0 8 2 6 - v=0 6 2 4
8	O-g	6	O-g	123313.9	333527	210213.1	Q,S	v=0 8 1 8 - v=0 6 1 6
8	O+g	6	O+g	126548.3	453636.9	327088.6	Q,S	v=0 8 2 7 - v=0 6 2 5
8	E-g	6	E-g	129686.3	348829.3	219143.1	Q,S	v=0 8 1 7 - v=0 6 1 5
9	E-g	7	E-g	143393.1	529543.4	386150.3	Q,S	v=0 9 2 8 - v=0 7 2 6
9	O+g	7	O+g	146933	426605.4	279672.5	Q,S	v=0 9 1 8 - v=0 7 1 6
9	O-g	7	O-g	142769.9	378674.7	235904.8	Q,S	v=0 9 0 9 - v=0 7 0 7
9	O-g	7	O-g	144124.7	530730	386605.3	Q,S	v=0 9 2 7 - v=0 7 2 5
9	E+g	7	E+g	139716.4	407484.2	267767.7	Q,S	v=0 9 1 9 - v=0 7 1 7
10	E+g	8	E+g	159366	462499.2	303133.2	Q,S	v=0 10 0 10 - v=0 8 0 8
10	E+g	8	E+g	161244	615637.9	454393.9	Q,S	v=0 10 2 8 - v=0 8 2 6
10	O-g	8	O-g	156105.1	489632.1	333527	Q,S	v=0 10 1 10 - v=0 8 1 8
10	O+g	8	O+g	160227.4	613864.2	453636.9	Q,S	v=0 10 2 9 - v=0 8 2 7
10	E-g	8	E-g	164162	512991.3	348829.3	Q,S	v=0 10 1 9 - v=0 8 1 7
10	E-g	8	E-g	160539.5	801693.7	641154.2	Q,S	v=0 10 3 7 - v=0 8 3 5
11	E-g	9	E-g	177049.8	706593.2	529543.4	Q,S	v=0 11 2 10 - v=0 9 2 8
11	O+g	9	O+g	181370.5	607976	426605.4	Q,S	v=0 11 1 10 - v=0 9 1 8
11	O-g	9	O-g	175899.7	554574.4	378674.7	Q,S	v=0 11 0 11 - v=0 9 0 9
11	O-g	9	O-g	178413.5	709143.4	530730	Q,S	v=0 11 2 9 - v=0 9 2 7
11	E+g	9	E+g	172478.9	579963	407484.2	Q,S	v=0 11 1 11 - v=0 9 1 9
12	E+g	10	E+g	192367.6	654866.9	462499.2	Q,S	v=0 12 0 12 - v=0 10 0 10
12	E+g	10	E+g	195635	811272.9	615637.9	Q,S	v=0 12 2 10 - v=0 10 2 8
12	O-g	10	O-g	188836.7	678468.8	489632.1	Q,S	v=0 12 1 12 - v=0 10 1 10
12	O+g	10	O+g	193859.2	807723.5	613864.2	Q,S	v=0 12 2 11 - v=0 10 2 9
12	E-g	10	E-g	198555.8	711547.1	512991.3	Q,S	v=0 12 1 11 - v=0 10 1 9

J

13	E-g	11	E-g	210654.5	917247.7	706593.2	Q,S	v=0 13 2 12 - v=0 11 2 10
13	O+g	11	O+g	215714.9	823690.8	607976	Q,S	v=0 13 1 12 - v=0 11 1 10
13	O-g	11	O-g	208768	763342.5	554574.4	Q,S	v=0 13 0 13 - v=0 11 0 11
13	O-g	11	O-g	212909.2	922052.7	709143.4	Q,S	v=0 13 2 11 - v=0 11 2 9
13	E+g	11	E+g	205177.9	785140.9	579963	Q,S	v=0 13 1 13 - v=0 11 1 11
14	E+g	12	E+g	225100.8	879967.6	654866.9	Q,S	v=0 14 0 14 - v=0 12 0 12
14	O-g	12	O-g	221501.7	899970.5	678468.8	Q,S	v=0 14 1 14 - v=0 12 1 12
14	E-g	12	E-g	232844.3	944391.5	711547.1	Q,S	v=0 14 1 13 - v=0 12 1 11
15	O-g	13	O-g	241367.5	1004710	763342.5	Q,S	v=0 15 0 15 - v=0 13 0 13
15	E+g	13	E+g	237807.7	1022949	785140.9	Q,S	v=0 15 1 15 - v=0 13 1 13

Table 3. PGOPHER peak assignment. 59 peaks for main BD isotope were fitted to get the rotational constants introduced in Table 1. Double prime (“) stands for the ground state and single prime (‘) stands for the excited state. E/O are the even and odd rotational states. v is the vibrational state.

The assigned peak list of 1-^{13}C-BD isotope

J'	Sym'	J"	Sym"	Observed	Calculated	Obs-Cal	Branch(ΔK,ΔJ)	v/J/Ka/Kc (final-initial)
5	Bg	3	Bg	73802.48	73801.281	1.199381	Q,S	v=0 5 0 5 - v=0 3 0 3
5	Ag	3	Ag	75689.98	75690.537	-0.55669	Q,S	v=0 5 1 4 - v=0 3 1 2
6	Ag	4	Ag	90143.58	90141.953	1.626743	Q,S	v=0 6 0 6 - v=0 4 0 4
7	Bg	5	Bg	104058.1	104055.98	2.1163	Q,S	v=0 7 1 7 - v=0 5 1 5
7	Bg	5	Bg	106446.66	106447.14	-0.481882	Q,S	v=0 7 0 7 - v=0 7 0 7
7	Ag	5	Ag	109289.54	109290.02	-0.482844	Q,S	v=0 7 1 6 - v=0 5 1 4
8	Ag	6	Ag	120036.45	120036.89	-0.440678	Q,S	v=0 8 1 8 - v=0 6 1 6
8	Ag	6	Ag	122710.62	122710.81	-0.19289	Q,S	v=0 8 0 8 - v=0 8 0 8
9	Bg	7	Bg	136004.41	136006.46	-2.052823	Q,S	v=0 9 1 9 - v=0 7 1 7
9	Bg	7	Bg	138927.72	138927.32	0.399411	Q,S	v=0 9 0 9 - v=0 7 0 7
9	Ag	7	Ag	142843.16	142843.22	-0.06086	Q,S	v=0 9 1 8 - v=0 7 1 6

Table 4. PGOPHER peak assignment. 11 peaks for 1-^{13}C-BD isotope were fitted to get the rotational constants introduced in Table 2. Double prime (“) stands for the ground state and single prime (‘) stands for the excited state. E/O are the even and odd rotational states. v is the vibrational state.

The assigned peak list of 2-^{13}C-BD isotope

J'	Sym'	J''	Sym''	Observed	Calculated	Obs-Cal	Branch(ΔK,ΔJ)
4	E+O-g	2	E+O-g	58825.15	58824.2762	0.8738	Q,S
5	E+O-g	3	E+O-g	75588.14	75586.9891	1.1509	Q,S
6	E+O-g	4	E+O-g	92318.53	92316.6828	1.8472	Q,S
6	E-O+g	4	E-O+g	94829.87	94828.9242	0.9458	Q,S
7	E+O-g	5	E+O-g	106484.44	106480.4264	4.0136	Q,S
7	E+O-g	5	E+O-g	109004.53	109006.2955	-1.7655	Q,S
7	E-O+g	5	E-O+g	112046.49	112045.6393	0.8507	Q,S
8	E+O-g	6	E+O-g	125648.12	125649.0828	-0.9628	Q,S
8	E-O+g	6	E-O+g	129248.29	129249.441	-1.151	Q,S
9	E+O-g	7	E+O-g	142234.51	142238.802	-4.292	Q,S

Table 5. PGOPHER peak assignment. 10 peaks for 2-^{13}C-BD isotope were fitted to get the rotational constants introduced in Table 2. Double prime (“) stands for the ground state and single prime (‘) stands for the excited state. E/O are the even and odd rotational states. v is the vibrational state.

7. References

1. Kroto, H.W. (1992). *Molecular Rotation Spectra*
2. *J. Chem. Soc., Faraday Trans. 2*, 1975,71, 812-826
3. J. Chem. Phys. 11, 27 (1943)
4. Landau, Lev Davidovich & Lifshitz, Evgeny Mikhailovich (1980) [1976]. *Statistical Physics*. Course of Theoretical Physics. 5 (3 ed.)
5. Kennard, E. H. (1927), "Zur Quantenmechanik einfacher Bewegungstypen", *Zeitschrift für Physik* (in German),
6. http://hyperphysics.phy-astr.gsu.edu/hbase/pauli.html
7. J. Kraitchman, Am. J. Phys. 21, 17 (1953)
8. *J. Phys. Chem.*, 1992, *96* (20), pp 7844–7857
9. Annual Rev. Anal. Chem. 2014.7:361-381
10. J. Chem. Phys. 148, 164302 (2018)
11. PNAS May 15, 2018 115 (20) 5072-5076
12. *J. Phys. Chem. A*, 2015, *119* (8), pp 1309–1314
13. *Science* 19 Aug 2011: Vol. 333, Issue 6045, pp. 1011-1015
14. J. Phys. Chem. A 2004, 108, 3367-3372110-12116.
15. Craig, N. C.; Groner, P.; McKean, D. C.; Tubergen, M. J. Int. J. Quantum Chem. 2003, 95, 837-852.Craig, N. C.; Davis, J. L.; Hanson, K. A.; Moore, M. C.; Weidenbaum, K. J.; Lock, M. J. Mol. Struct. 2004, 695-696, 59-69.
16. Craig, N. C.; Hanson. K. A.; Pierce, R. A.; Saylor, S. D.; Sams, R. L. J. Mol. Spectrosc. 2004, 228, 401-413.
17. Craig, N. C.; Hanson, K. A.; Moore, M. C.; Sams, R. L. J. Mol. Struct. 2005, 742, 21-29.
18. *J. Phys. Chem. A*, 2006, *110* (23), pp 7461–7469
19. *J. Phys. Chem. A*, **2015**, *119* (8), pp 1309–1314
20. PGOPHER, A Program for Simulating Rotational, Vibrational and Electronic Spectra, C. M. Western, *Journal of Quantitative Spectroscopy and Radiative Transfer*, 186 221-242 (2016)
21. D. J. Marais, N. Sheppard and B. P. Stoicheff, Tetrahedron, 1962, 17, 163